AD-A038 423 PURDUE UNIV LAFAYETTE IND PROJECT SQUID HEADQUARTERS F/G 20/4
TEMPERATURE, CONCENTRATION VELOCITY AND TURBULENCE MEASUREMENTS--ETC(U)
DEC 76 S LEDERMAN, A CELENTANO, J GLASER N00014-75-C-1143
UNCLASSIFIED SQUID-PIB-34-PU NL

1 OF 1
AD A038423

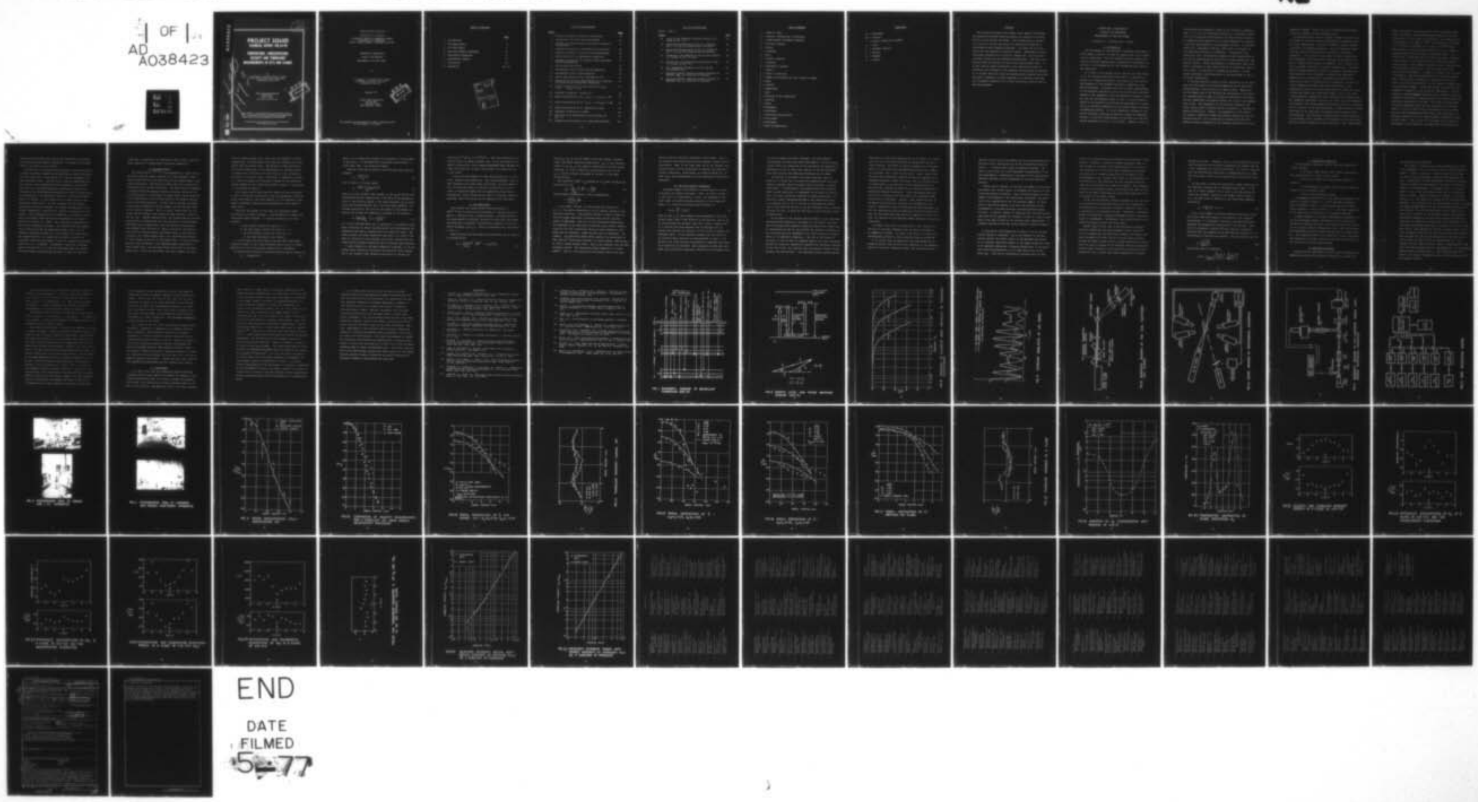

END
DATE
FILMED
5-77

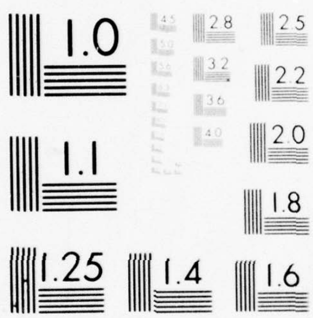

MICROCOPY RESOLUTION TEST CHART
NATIONAL BUREAU OF STANDARDS-1963-A

PROJECT SQUID

TECHNICAL REPORT PIB-34-PU

TEMPERATURE, CONCENTRATION, VELOCITY AND TURBULENCE MEASUREMENTS IN JETS AND FLAMES

BY

S. LEDERMAN, A. CELENTANO AND J. GLASER
POLYTECHNIC INSTITUTE OF NEW YORK
FARMINGDALE, NEW YORK

PROJECT SQUID HEADQUARTERS
CHAFFEE HALL
PURDUE UNIVERSITY
WEST LAFAYETTE, INDIANA 47907

Project SQUID is a cooperative program of basic research relating to Jet Propulsion. It is sponsored by the Office of Naval Research and is administered by Purdue University through Contract N00014-75-C1143, NR-098-038.

Technical Report PIB-34-PU

PROJECT SQUID

A COOPERATIVE PROGRAM OF FUNDAMENTAL RESEARCH
AS RELATED TO JET PROPULSION
OFFICE OF NAVAL RESEARCH, DEPARTMENT OF THE NAVY

TEMPERATURE, CONCENTRATION VELOCITY AND TURBULENCE MEASUREMENTS IN JETS AND FLAMES

by

S. Lederman, A. Celentano and J. Glaser
Polytechnic Institute of New York
Farmingdale, New York

December 1976

Project SQUID Headquarters
Chaffee Hall
Purdue University
West Lafayette, Indiana

H

Table of Contents

List of Illustrations

List of Illustrations

Cont'd - Page 2

List of Symbols

c = speed of light

C = constant (calibration or otherwise)

d = random sample of Doppler frequency

e = electron (charge)

E = energy

f = frequency

G = gain

h = Planck's constant

I = intensity

k = Boltzmann's constant

ℓ = length

n = index of refraction

N = number of scatterers per unit volume or number

P = power

R = resistor

T = temperature

t = time

u = velocity in the x-direction

V = velocity

θ = angle

ν = wavenumber

η = efficiency

σ = scattering cross-section

Ω = solid angle

λ = wavelength

χ = Raman susceptibility

Subscripts

as = antistokes

coh = coherent

i = initial condition or number

L = laser

o = incident, optical

p = photon

q = quantum

s = stokes

Abstract

The recently developed Laser Raman, Laser Doppler Velocimetry and Coherent Antistokes Raman Scattering are applied to the diagnostics of flow fields and flames. The concentration of species in a cold jet, and the velocities are measured and compared to measurements using standard techniques. The Raman and LDV techniques are then applied to diffusion flames. Experimental results concerning concentration of species, temperature, velocities and turbulent intensities are obtained simultaneously. The latter are obtained from the LDV data as well as the concentration data. It is seen that by proper processing of the concentration data an indication and a measure of the turbulent intensity may be obtained. It is further shown that from the simultaneously acquired concentration data a parameter of major importance in turbulence modeling, the "mixedness" parameter or the cross correlation function may be directly measured.

TEMPERATURE, CONCENTRATION VELOCITY AND TURBULENCE MEASUREMENTS IN JETS AND FLAMES

S. Lederman, A. Celentano and J. Glaser

1. Introduction

The development of new diagnostic techniques applicable to fluid dynamic research, has been an ongoing task in our laboratory for many years. With the funding by Project Squid this task was directed towards optical nonintrusive techniques, applicable to the diagnostics, of flow fields propulsive devices, and combustion.

As a result of the energy crisis, and the fact that almost all of the energy derived from fossil fuels is obtained as a product of a combustion process, the interest in the detailed understanding of the phenomena involved in combustion, has been revitalized. It became clear that a better understanding of the processes involved is vital not only for more efficient designs of the combustors, with the associated savings in fuels, but from the environmental point of view, it could provide an answer to the problem of protecting the environment by a reduction or a possible elimination of the harmful exhaust emissions of combustion systems. It is well known that contrary to the highly developed technology in practical design of combustion systems, a scientific understanding of the details of the combustion processes is still in its infancy. However, recent in-

vestigations and exchanges of views in the scientific community (Ref. 1,2,3,4,5) have contributed greatly to a systematic definition of the problems and delineation of some particular aspects of combustion which appear to be of major importance in reaching a detailed understanding of the phenomena involved. It has been found that a phenomenon exerting a great deal of influence on the combustion processes is turbulence. A knowledge of the turbulence level, instantaneous temperature and concentration of the species involved may be very useful in understanding the combustion process. Modern developments in nonintrusive laser diagnostic techniques of flow fields could be of significant value in this context, if applicable to combustion processes. As mentioned previously, nonintrusiveness of the measurement is one of the major requirements.

It has been generally agreed by most researchers in the field that the first aspect of nonintrusiveness and by the same token noninterference, can be best met by optical means. Neglecting for the moment some of the difficulties encountered in the practical implementation of some of the optical measurement techniques, one must immediately distinguish between the internal and external flow fields. The diagnostics of the external combustion flow field, having almost unlimited optical accessibility, presents no special difficulties. However, the diagnostics of the flow of the internal combustion chamber may present problems not only of accessibility but also of potentially disruptive and flow disturbing features introduced by the necessary modifications of the

combustion chamber. These have to be considered and minimized as much as possible in each individual case.

As mentioned above, optical methods represent the best hope at present of achieving the best measurement in combustion with the least interference. There are a number of optical methods utilizable for diagnostic purposes. They are generally associated with particle and molecular scattering, or molecular absorption. In the last few years some of these methods have been developed to the point where they are now incorporated as part of commercially available instruments. Most, however, are only utilizable at present in research laboratories. The major optical methods presently utilized for diagnostic purposes are Mie scattering in LDV, Rayleigh, in density and temperature, fluorescence in concentration, absorption in concentration, vibrational Raman in concentration and temperature, and most recently coherent Antistokes Raman scattering which is very promising by virtue of its very strong signal of about six orders of magnitude higher than vibrational Raman. Most of the above listed diagnostic methods have their advantages and disadvantages. The theoretical background of most of the above scattering phenomena are different and require generally different analytical treatment. They all however can be characterized by a common convenient parameter known as the equivalent scattering cross-section in units cm^2/Steradian. This parameter, besides being a strong function of the phenomenon itself, depends on the character of the scattering particle and the frequency of the illuminating light, among others.

These scattering cross-sections vary over an extremely large range. Typically, the scattering cross-section for the Mie scattering is in the range of $10^{-8} cm^2$/Ster. for absorption and fluorescence of the order of 10^{-20}, for Rayleigh of the order of $10^{-27} cm^2$/Ster. and Raman of the order of $10^{-30} cm^2$/Ster. CARS may have a scattering cross section of up to 6 orders of magnitude higher than the regular vibrational Raman. It is obvious that a technique with the larger equivalent scattering cross section is to be preferred over the ones with smaller cross sections. This, however, would be a great simplification of the problem at hand since it involves only one of the characteristic parameters. A number of criteria have to be met in performing a particular measurement in a particular situation. Some of these techniques are limited in sensitivity (small scattering cross section) but are capable of spatial and time resolution (Raman). Others may be more sensitive but are incapable of spatial or time resolution (absorption). Any information concerning spatial resolution may be obtained after considerable accumulation of absorption data and sophisticated computational processing of the same. The other above-mentioned scattering phenomena except the Mie scattering are generally superior as far as sensitivity is concerned relative to Raman but have other disadvantages which limit their usefulness. A thorough discussion of all of these methods is beyond the scope of this report. Since in the last few years in the course of development of new diagnostic techniques for fluid dynamic re-

search utilizing lasers our efforts were directed at Laser Raman Scattering and Laser Doppler anenometry, this paper will discuss some of the results of our efforts.

Specifically, our attention was focussed on the applicability of Raman scattering towards the determination of specie concentration and temperature, among others, in a mixing axisymmetric jet and air-methane flame. This particular task was undertaken with the explicit aim of demonstrating the feasibility, proving the applicability, and establishing the technology of remote, instantaneous and simultaneous determination of specie concentration and temperature of the individual specie in a flow field without mechanical probes. In this report after a short review of the spontaneous Raman effect, the LDV technique and the Coherent Antistokes Scattering technique, an attempt is being made to determine temperature, concentration, velocity in coaxial jets and flames. After demonstrating this capability, an attempt is being made to determine simultaneously the concentration of several species of interest in a flame, their individual temperatures as well as the turbulence intensity. The concentration and temperature is obtained using the spontaneous Raman effect, and the turbulent intensity by means of a L.D.V.. Using the concentration and temperature data, an attempt will be made to extract the flucuation intensity and compare it with the intensity as obtained using the L.D.V. techniques. Furthermore, some data concerning specie concentration in a flame are discussed using the coherent antistokes Raman scattering method which, in spite of some dis-

advantages as compared to the spontaneous Raman effect, may be of major importance in applications concerning combustion.

2. The Raman Effect

The Raman Effect[6,7,8,9,10] is the phenomenon of light scattering from a material medium, whereby the light undergoes a wavelength change and the scattering molecules an energy change in the scattering process. The Raman scattered light has no phase relationship with the incident radiation. The Raman shifts correspond to energy differences between discrete stationary states of the scattering system. Classically, the Raman Effect can be described as the modulation of the scattered light by the internal motions of the scattering molecules. In this kind of analogy, the Raman lines would correspond to the side bands, and the Rayleigh light to the carrier frequency. This, of course, would result in the Stokes and Anti-Stokes lines having the same intensity, which is not the case. Quantum theoretically, the incident photons collide elastically or inelastically with the molecules to give Rayleigh and Raman lines, respectively, with the inelastic process much less probable than the elastic. When an inelastic collision occurs with the incident photon furnishing energy to the molecule raising it to a higher energy level, the scattered photon being of lower energy, gives rise to the Stokes line. If the scattering molecule gives up energy to the impinging photon and moves to a lower energy state, the scattered photon gives rise to the Anti-Stokes line. Since the Anti-Stokes line must originate in mole-

cules of higher energy level, which are less abundant at normal temperatures, the Anti-Stokes lines would be expected to be much weaker than the Stokes lines. The process of light scattering can thus be visualized, as the absorption of an incident photon of energy E by a molecule of a given initial state, raising the molecule to a "virtual" state, from which it immediately returns to a final stationary state emitting a photon of the difference energy between the two states and incident energy E. The process is illustrated in Figure 1.

This general qualitative behavior, holds for the vibrational as well as rotational transitions, with the appropriate selection rules, which tend to limit what appears to be an extremely large number of possible transitions and consequently large number of Raman lines.

Since for the purpose of this work the vibrational Raman scattering is of direct interest, it is worthwhile to examine the vibrational Raman response. It consists essentially of three branches:

a) The intense Q branch for which $\Delta J = 0$

b) The much weaker O branch for which $\Delta J = -2$

c) The much weaker S branch for which $\Delta J = +2$ of the same intensity as the O branch.

It can be shown that only about 1% of the total vibrational intensity resides in the O and S branches and as such is of minor importance as far as the present application is concerned.

In quantitative terms the scattered intensity may be written as:

$$I_{s'} = CI_O N_T \sigma f(T) \Omega . \tag{1}$$

where C is a calibration constant of the system, N is the number of scatterers, σ is the equivalent scattering cross-section, Ω solid angle, and ℓ the scattering length.

Equation 1 written in terms of the scattered signal photons, becomes:

$$n_s = \frac{E_o N\sigma.\ell\Omega\eta_o}{E_p} \tag{2}$$

and in terms of a voltage signal

$$V_s = \frac{E_o N\sigma.\ell.\Omega.\eta_o\eta_q.G.e.R}{E_p.t.} \tag{3}$$

where E_o is the incident laser energy, η_o and η_q the optical and quantum efficiencies respectively, G the gain of the photomultiplier, e the electron charge, R the load resistance, E_p the energy of the scattered photon, and t the laser pulse duration. In thermal equilibrium, the ratio of the Stokes to anti-Stokes intensity can provide the temperature according to the equation:

$$T = \frac{h\nu c}{k}\left[\ln\frac{I_s}{I_{as}} + 4\ \ln\ \left(\frac{\nu_o+\nu}{\nu_o-\nu}\right)\right]^{-1} \tag{4}$$

It is clear from the above that in principle it is possible using Raman scattering to obtain instantaneously and simultaneously the temperature and specie concentration in a mixture of gases. The former because the Raman transitions take place in a time of the order of fractions of pico-seconds, the latter, because both the Stokes and anti-stokes intensities may be obtained simultaneously.

A major drawback of the Raman diagnostic technique, is the extremely small equivalent scattering cross-section, which depending on the incident laser frequency and specie of interest may

vary from $10^{-31} cm^2/sr$ to $10^{-28} cm^2/sr$. This low scattering cross-section forces not **only** a minimum limit on the resolvability of specie concentration, which **remains relatively high, and may** also limit the resolution of small fluctuations in concentration in a flow field.

A recent new development in Raman Spectroscopy may, in some cases, improve these conditions. This new development, known as CARS (Coherent-Anti-Stokes Raman Scattering), has been shown to have an equivalent Raman scattering cross-section of up to 6 orders of magnitude higher than the spontaneous Raman Effect. Consequently, specie concentration levels, of several orders of magnitude lower than before can be expected to be resolvable.

3. The CARS Effect

The coherent Anti-Stokes Raman Scattering Effect or CARS[11,12] may be qualitatively described as a process by which a photon ν, interacts with a tunable photon, ν_2 (Stokes photon of the given specie of interest) through the third order non-linear susceptibility to generate a polarization component of the Anti-Stokes frequency $\nu_3 = 2\nu_1 - \nu_2$. This is diagrammatically represented in Fig. 2.

Quantitatively the Anti-Stokes scattered power can be shown to be represented by:

$$P_{as} = \frac{2.77 . 10^{-3}}{n_{as}^4 \lambda_{as}^2} \left(\frac{\ell_{coh}}{A}\right)^2 \times [N\gamma]^2 P_L^2 P_2 \qquad (5)$$

where P_{as}, P_L, P_s are the powers of the Anti-Stokes, incident laser, and Stokes radiation respectively, ℓ_{coh} is the coherence length in cm, n_{as} is the index of refraction at the Anti-Stokes frequency, A is the interaction cross-sectional area in cm^2 λ_{as} is the Anti-Stokes wavelength in cm and χ is the Raman Susceptibility.

The coherence length ℓ_{coh} defined as $\pi/_{\Delta k}$ where $\Delta k=2k_1-k_2-k_3$ may be written as:

$$\ell_{coh} = \frac{\pi c}{\nu_{vibr}^2}\left[2\,\frac{\partial n}{\partial \nu} + \nu_L\,\frac{\partial^2 n}{\partial \nu^2}\right] \tag{6}$$

and the Raman Susceptibility χ may be expressed as

$$\chi = \frac{2\pi^2 c^4}{h\omega_L \omega_s^3 \Gamma_R}\,\frac{d\sigma}{d\Omega} \tag{7}$$

It is evident from Eq. (5) that unlike the relation of Eq. (1), the specie concentration is not linearly related to the scattered radiation. This negative feature of CARS is offset by the much higher equivalent scattering cross section (several orders of magnitude), than that of the spontaneous Raman Effect. The magnitude of the equivalent scattering cross section, however, cannot be the only criterion by which the above diagnostic techniques may be evaluated. Other features must be considered. For example: the spontaneous Raman Effect permits the measurement of many species[13] which may be present in a given system, simultaneously using a single primary laser. This is not possible with the CARS diagnostic method. The spontaneous Raman diagnostics is single ended[14]. That is, the transmitter and receiver may use the same

optics or may be located in proximity to each other. This is not possible with CARS except by using remotely located reflecting mirrors. CARS, on the other hand, due to its coherent high intensity beam, may be advantageous in systems with high background illumination, fluorescence, or radiation which may, in some cases, make measurements with the spontaneous Raman Effect impossible.

4. The Laser Doppler Anemometer

The Laser Doppler velocitymeter, as indicated by its name, is based on the Doppler principle. Thus, if a small volume in a flow field is illuminated by a laser, the frequency of the laser light scattered by moving particles in the volume will appear to a receiving stationary photo-detector as

$$f_D = f_o \pm \frac{n_o V}{\lambda_o} \cdot (\bar{e}_s - \bar{e}_i) \tag{8}$$

where f_o and λ_o are the frequency and wavelength of the illuminating laser light, $\bar{V}$ the velocity of the particle, and $\bar{e}_s$ and $\bar{e}_i$ the scattered and incident light unit vectors, respectively. It is obvious from this equation that in principle one can measure the velocity of a particle if one is able to measure the frequency shift. If one therefore assumes that the motion of the particle whose velocity is being measured is equal to the motion of the fluid in which the particle is immersed the motion of the fluid can be measured. This assumption can be made only under very restrictive conditions, which will be discussed later.

As with the Raman scattering technique, the Laser Doppler velocitymeter has been very highly developed in the last decade. A major source of information on the LDV theory and operation is References 15 and 16, where most aspects of the LDV technology have been treated, and additional references can be found.

In contrast to the Raman scattering technique, which is molecular in nature and is essentially omnidirectional the Laser Doppler technique, which is based on Mie scattering, is highly directional. In other words, while Raman scattering intensity under certain conditions is independent of the angle of observation, the other scattering technique is highly directional, exhibiting a highly pronounced maximum in the forward direction. It is obvious that as far as the LDV is concerned the forward lobe of the radiation pattern is the most desirable from a variety of points of view, of which not the least is the favorable signal-to-noise ratio.

In the course of the present research effort in our laboratory concerning laser diagnostic techniques of flow fields, the problem of resolving high frequency turbulence spectra was looked into. In considering the LDV for this problem the question of whether or not the solid particle suspended in the fluid follows the streamlines is of fundamental importance. How far do the results of velocity, as well as that of frequency spectra of tracer particles, provide the requisite information regarding the turbulent structure of the flow field? This question must be answered through careful analysis and consideration. The underlying precept permitting LDV

application to flow field diagnostics is, of course, the assumption that the scattering particles are moving with the local fluid velocity. The effect of particle dynamics on the performance of an LDV have been considered analytically by a number of researchers (Ref. 17-20) in the field. Yanta, using a generalized drag coefficient examined the particle dynamics in an expanding supersonic nozzle and noted a lag in velocity directly proportional to the diameter of the scattering particle. Tchen and Soo examined the behavior of a particle subjected to homogenous isotropic turbulence. Their conclusions were that the particle diffusivity was the same as the Lagrangian eddy diffusivity of turbulence. However, later studies by Soo, experimental and analytical, based on the "probability of encounter" showed that these two diffusivities were different and that the seed particles do not generally follow fluid particles. Even for very small particles which are expected to follow the flow, the increase in flow Reynolds number decreases the particle diffusivity.

In Figure 3 the ratio of the particle to gas velocity as a function of turbulent frequency with the particle diameter <u>a</u> as a parameter is shown. In Figure 4 the effect of 2 particles simultaneously present in the scattering volume is presented.

It is evident from the above that the relationship of the frequency spectra from an LDV to the turbulence of the medium is limited to the lower frequency region, that limitation being a

function of the size of the majority of the scattering particles. This puts also a restriction on the use of naturally occurring particulates because their sizes are generally unknown. The above suggests that for a more meaningful interpretation of the LDV measurements, a monitoring of the sizes of the particulates should be carried out and incorporated in the data reduction process.

Careful choice, however, of the size and number of scatterers does permit one, within limits, to determine the velocity of the fluid and turbulent intensity. Since the major problem in Laser Doppler velocitymetry is the acquisition, processing, and handling of the acquired data, not the principle itself, it would serve no particular purpose to go into the different optical arrangements or the many electronic processing methods being utilized. It should, however, be mentioned that the dual-scatter type which can be operated in a forward, as well as a back scatter mode is the type utilized in our and many other laboratories. A schematic diagram of the dual scatter system is shown in Figure 5

At this point a few remarks are in order as far as the dual scatter system is concerned. Due to the symmetry of the dual scatter system, the output current of the photodetector placed at an arbitrary angle with respect to the sample volume will have an AC component possessing a frequency proportional to the particles velocity perpendicular to the input optics axis of symmetry (U_p). This can be visualized by realizing that the dual

beam at the intersecting point generates an interference fringe pattern. Passage of a particle through successive light and dark fringes at the above interference pattern will result in the intensity of the scattered light displaying a sinusoidal variation with a frequency equivalent to the doppler shift corresponding to U_p. Because this signal is now independent of the direction of the wavevector for the scattered radiation, light may be collected over large solid angles. The subsequent increase in the signal-to-noise ratio allows this mode of operation to be used in situations for which only single particles are present in the sample volume.

In the case of multiple scatterers present at the same time, the sinusoidal waves mentioned above will be an aggregate of intefering waves as indicated in Figure 4 and will result in an ambiguity in the measured velocity. Therefore, a sparingly seeded flow field and a properly designed electronic processing system is recommended. Furthermore, each situation must be examined for optimal results and least error.

Another type of error, due to the statistical biasing of velocity information, has been examined in Refs. 21 and 22. If it is assumed that the particulate density will remain constant throughout the flow, the rate at which particles pass through the sample volume will be a linear function of velocity. This will cause a biasing of the measured velocity distribution towards higher velocities, since particles traveling at these speeds will have a larger than normal probability of passing

through the volume. Tiederman, Ref. 21, has considered the situation in which the true velocity distribution is gaussian and the u and v components are totally correlated. The results indicated that for distributions possessing a standard deviation of under 15% of the mean, errors in the measured mean velocity were under 2%.

At this point it should be noted that a simple indication of the turbulent intensity may be obtained using an LDV. In the case of a single component LDV as used in our laboratories defining the turbulent velocity in the normal fashion ($\bar{u}=u+u'$), i.e., the mean value in addition to the fluctuating component, one obtains,

$$f_d = \frac{2 \sin \theta/2}{\lambda_o} (\bar{u} + u') \tag{9}$$

With a large number of velocity samples N taken over a period of time large with respect to the period of the turbulent fluctuations, it is possible to develop a histogram which will represent the probability distribution of the velocity. From this it is possible to obtain the mean velocity, turbulence level and from the skewness of the distribution determine if the fluctuations of velocity are gaussian. The mean velocity will be

$$\bar{u} = \frac{\lambda_o \sum_i f_i d_i}{N 2\sin^{\theta}/2} \tag{10}$$

and the RMS value of turbulence

$$(u'^2)^{\frac{1}{2}} = \frac{\lambda_o}{2\sin^{\theta}/2}\left[\frac{\sum_i^N f_i (d_i)^2}{N-1} - \frac{(\sum_i^N f_i d_i)^2}{N(N-1)}\right]^{\frac{1}{2}} \tag{11}$$

5. Experimental Apparatus

The experimental apparatus used in this work consisted of 4 basic systems:

a) The basic Raman System used to obtain temperature and concentrations of a flow field or flame.

b) The L.D.V. System for velocity and turbulent intensity.

c) The CARS System to obtain small traces of unburned methane in an air methane flame.

d) The jet and combustion system.

A diagramatic representation of the complete experimental apparatus is shown in Figures 6, 7 and 8 and some photographic views in Figures 9 and 10. A full description of the experimental apparatus is given in Refs. 7, 13. The basic components of the apparatus are indicated in the schematic diagrams.

A common component in the above experimental arrangements is the data processing system, consisting of a data acquisition, storage and computing facility. This system allows the acquisition of a large amount of experimental data, store the raw data, and subsequently retrieve, analyze and present in a proper manner. This apparatus permits the acquisition of data concerning and temperature of several species in the flow field as well as the velocity of the flow simultaneously.

6. Experimental Results

Using the above experimental facility, specie concentration, temperature velocity and turbulent intensity of a coaxial jet

and flame have been obtained.

Thus Figure 11 presents the average concentration of CO_2 in an axisymmetric jet, as obtained using a limited number of samples. Figure 12 presents a velocity profile on the same jet using several measurement techniques and comparing the same. Conceptually, the LDV measurements should be extremely accurate, because the measurement of velocity is essentially reduced to the measurement of frequency, which, as is well-known, is one of the measurements which can be accomplished most accurately. However, problems in seeding, in data processing, etc., may reduce the accuracy of the velocity being measured. It is obvious that the LDV obtained velocity is larger the outer portions of the jet than those obtained using alternate methods. Part of this difference can be traced to the "statistical biasing" of the LDV which results from possible non-uniform seeding of the flow field in particular when the flow field is turbulent in nature, part from the nature of the electronic processing system which is using in this case a high pass filter, thus reducing the ability to measure small velocities, and partly from the fact that the scattering particulates were injected into the jet fluid upstream of the exit orifice, and no effort was made to seed the surrounding air. Thus, towards the outer edge of the jet, where a large portion of the fluid has been entrained from the surrounding air, the particulate density becomes extremely small. (The scatterers may, due to inertia, not acquire the local velocity) and the acquisition of data becomes tedious.

After identification of the possible sources of error involved in the measurements, a series of tests were conducted on a coaxial jet with the ratio of the outer to inner jet areas $(A_o/A_i) = .26$ and $U_o/U_{in} = .45$. The results are shown in Figure 13. Figure 14 presents the turbulent intensity corresponding to velocity profiles shown in Figure 13.

In Figures 15 and 16, radial distribution of velocity profiles for $A_o/A_i = 1.28$ and $U_o/U_i = .5$ and $U_o/U_i = .74$ respectively are shown. A fairly good agreement with theory and other experimental data is readily evident.

Some radial distributions of velocity in a methane air flame are shown in Figure 17 and the turbulent intensity in Figure 18. Figure 19 and 20 present examples of measurement concentration and temperature profiles in an air methane flame respectively. The above velocity concentration and temperature data have not always been obtained simultaneously. However the recent expansion of our data acquisition and processing systems, permit the routine acquisition of such data simultaneously. As an example of this new capability the data as shown in Figures 21, 22, 23, 24 and 25 have been obtained simultaneously. Thus Figure 21 presents a velocity profile in a flame at X/D = 5,2 with the corresponding computed turbulent intensity. Figure 22 the N_2 concentration in the same flame at the same X/D and the corresponding concentration fluctuation, Figure 23 the CO_2 concentration and concentration fluctuation and Figure 24 and 25 the corresponding N_2 and CO_2 temperatures and their fluctuations.

If one compares the N_2 concentration and the corresponding temperature profiles, somewhat symmetrical distributions are evident. This is not the case for CO_2. Here the CO_2 concentration is higher at the right hand side of the distribution profile, while the corresponding temperature is lower. This is perfectly natural since cold CO_2 was introduced into the flame, and the higher CO_2 concentration would naturally correspond to a lower temperature. This has been actually observed visually in the flame.

As a result of the fact that the data were obtained simultaneously, a parameter of importance in turbulence modeling may be obtained. This parameter referred to as chemical "mixedness" is shown in Figure 26 and was obtained from the concentration data of Figures 21 and 23. Finally in Figure 27, and 28 two calibration curves for Methane and Hydrogen are given as obtained using the CARS apparatus shown in Figure 7. An attempt to obtain the traces of unburned methane in a flame as a function of axial distance from the exit of the jet using CARS was partially successful. However the ruby laser used for that purpose has broken down and must undergo major repairs.

7. Conclusions

It is quite clear that the vibrational Raman scattering technique and the Laser Doppler Velocimeter are capable of providing nonintrusively most of the basic information regarding flow fields. The limitations of those techniques appear to be more in the practical implementation than in the basic concepts.

Thus, there is a lower limit of resolution capability of the Raman scattering technique due to a combination of factors such as the available primary laser power, the number of scatterers in the sample volume, the number of background photons, etc.. A very convenient parameter to assess the capability of a system is the "feasibility index", Ref. 23. This index was defined as $X = NL\sigma_o \Omega e$ where N is the number density of the scatterers per cm^3, L is the length of the sample in the direction of the laser beam, σ_o reference cross section, and Ω and e the solid angle and optical efficiency, respectively. The min. feasibility index for a 1 j Ruby laser single pulse is approximately 10^{-15}. Thus, for a situation where this index is below 10^{-15} a 1 joule single pulse laser would not provide the desired information. An increase in the laser energy or any of the other factors may be necessary. There is, however, a limit on the laser energy one may apply. The laser energy density should be below the breakdown threshhold which for Ruby and air appears to be around 10^{10} Watts/cm^2. As far as the LDV is concerned, it is without doubt one of the major diagnostic developments for fluid dynamic research attributable to lasers. It reduces velocity measurements to the measurement of frequency, independent of the thermodynamic state of the medium, capable of yielding accuracies far in excess of any other method, and most importantly, without disturbing probes and the measurement is accomplished remotely.

It is evident from the above that the optical methods and particularly LDV and spontaneous Raman scattering while not free from difficulties and limitations, are essentially the two most important diagnostic techniques applicable in general to flow fields as well as to external and internal combustion. The nonintrusive, remote, specific, pointwise, time and space resolution capabilities, are the major assets of these diagnostic techniques. The low scattering cross section of the Raman diagnostic techniqe, which is the source of major difficulties, may be the price one has to pay for the other advantages. However, improvement in the collector optics and data acquisition equipment, including the phtomultiplier performance, may alleviate some of the difficulties. The recent developments in tunable dye lasers may also provide some possibilities in improving the signal to noise ratio by permitting to shift into a more favorable frequency band in terms of background noise. The further development of the CARS method, among others being explored at the moment, may also provide a means of enhancing the optical nonintrusive diagnostic methods in flow fields and combustion.

References

1. Goulard, R., "Combustion Measurements in Jet Propulsion System", Project SQUID Workshop PU-RI-76, Dec. 1975.

2. Lapp, M., Hartley, D. L., "Raman Scattering Studies of Combustion", Combustion Science & Technology, Vol. 13, pp. 199-210, 1976.

3. Glassman, I., Sirignano, W. A., (August, 1974), Summary report of the Workshop on Energy Related Basic Combustion Research. Sponsored by N.S.F. Princeton Univ., Rep. No. 1177.

4. Murthy, S.N.B., Editor, "Turbulent Mixing in Nonreactive and Reactive Flows", Project SQUID Headquarters, Plenum Press, N. Y. 1974.

5. Gupta, R.N., Wakelyn, N.T., "Theoretical Study of Reactive and Nonreactive Turbulent Coaxial Jets", NASA TN D-8127, Aug. 1976.

6. Placzek, G., "Rayleigh Streuung and Raman Effect", Hanbuch der Radiologie, Leipzig: Akademische Verlagegesellshaft VI, 1934.

7. Lederman, S., "Modern Diagnostics of Combustion", AIAA Paper No. 76-26.

8. Herzberg, G., "Spectra of Diatomic Molecules", D. Van Nostrand Co., N. Y. 1963.

9. Widhopf, G., Lederman, S., "Specie Concentration Measurements Utilizing Raman Scattering of a Laser Beam", AIAA J. 9-1971., PIBAL Rep. No. 69046, Nov. 1969.

10. Lapp, M. and Penny C., Editors, "Laser Raman Gas Diagnostics", Plenum Press N.Y., and London 1974.

11. Begley, R.F., Harvey, A.B., and Byer, R.L., "Coherent Anti Stokes Raman Spectroscopy Appl. Phys. Letters Vol. 25, No. 7, 1974.

12. Regnier, P.R., Moya, F., Taran, J.P.E., "Gas Concentration Measurement by Coherent Raman Antistokes Scattering", AIAA Paper No. 73-702, July 1973.

13. Lederman, S., Bornstein, J., Celentano, A., Glaser, J., "Temperature Concentration and Velocity Measurements in a Jet and Flame" Proj. SQUID, Tech. Rep. PIB-33-PU.

14. Lederman, S., Bloom, M., "The Raman Effect and Air Pollution Measurements, J. Env. Syt., Vol. 2(4) 1972.

15. Stevenson, W.H., Thompson, H.D., Editors: "The Use of Laser Doppler Velocimeter For Flow Measurements", Proceedings of a Workshop Project SQUID, 1972.

16. Thompson, H.D. and Stevenson, W.H., Editors: "Second International Workshop on Laser Velocimetry", Vol. I and Vol. II, Project SQUID, 1974.

17. Duvost, F. "Scattering Phenomena and Their Application in Optical Anemometry", Jo. of Appl. Math. & Physics, Vol. 24 1973.

18. Yanta, W. J., "Measurement of Aerosol Size Distr. with an L.D.V., AIAA Paper 73-705.

19. Soo, S.L., "Fluid Dynamics of Multiphase Systems", Blaisdell 1972.

20. Khosla, P.K. and Lederman, S., "Motion of a Spherical Particle in a Turbulent Flow", PIBAL Report No. 73-72, Nov. 1973.

21. McLaughlin, D.K., Tiederman, W.G. "Biasing Correction for Individual Realization of Laser Anemometer Measurements in Turbulent Flow". The Physics of Fluids, Vol. 16, 1973.

22. Kried, D.K., "Laser Velocimeter Measurements in Nonuniform Flow: Error Estimates". Applied Optics, Vol. 13, No. 8, August 1974.

23. Goulard, R., "Laser Raman Scattering Applications", J. Quant. Spectr. Radiat. Transfer, Vol. 14, pp. 969-974, Pergamon Press 1974.

24. Mons, R. F. and Sforza, P. M.: "Turbulent Heat and Mass Transfer in Axisymmetric Jets". PIBAL Report No. 71-14, May 1971.

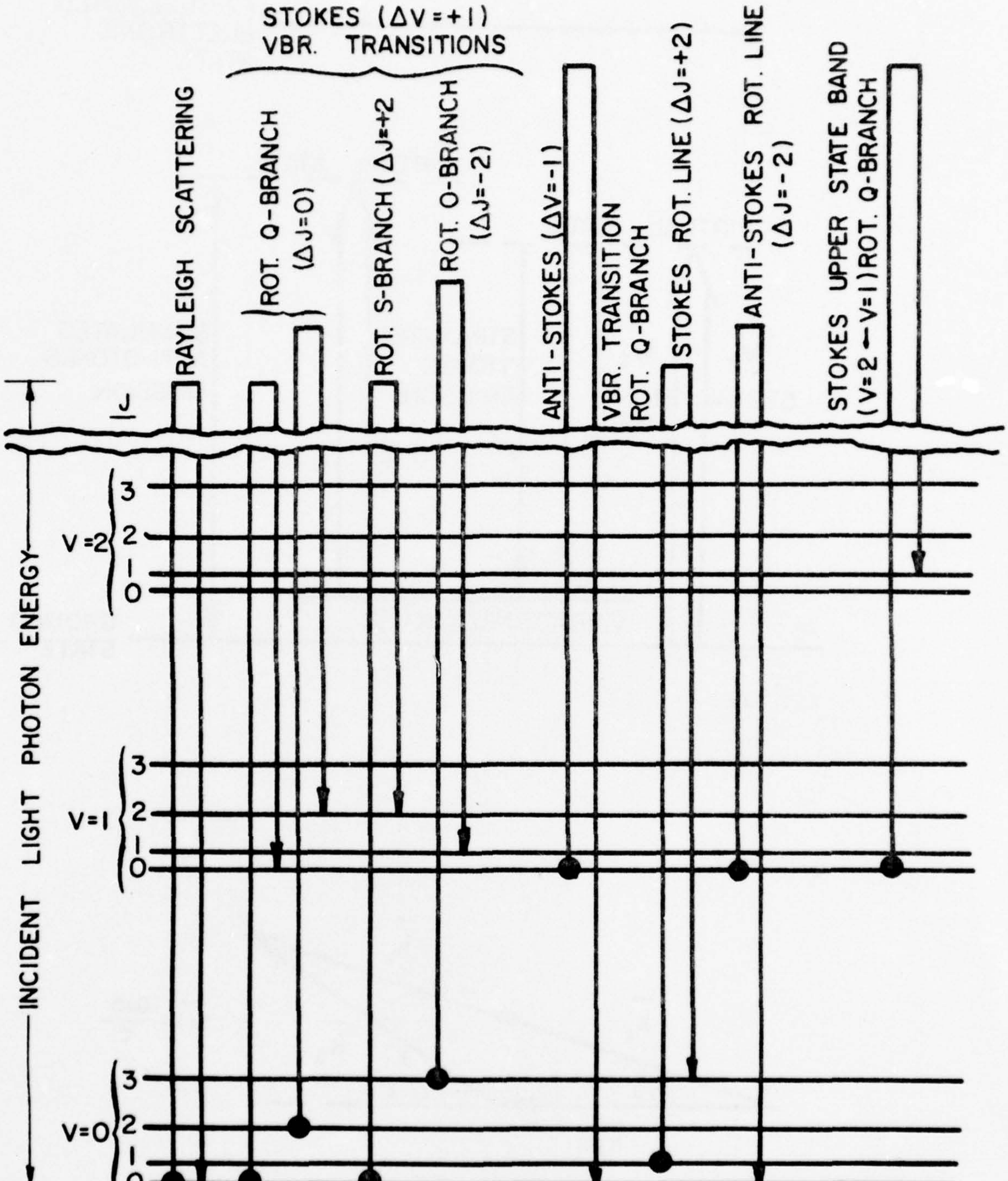

FIG. 1 SCHEMATIC DIAGRAM OF MOLECULAR TRANSITION (REF. 10)

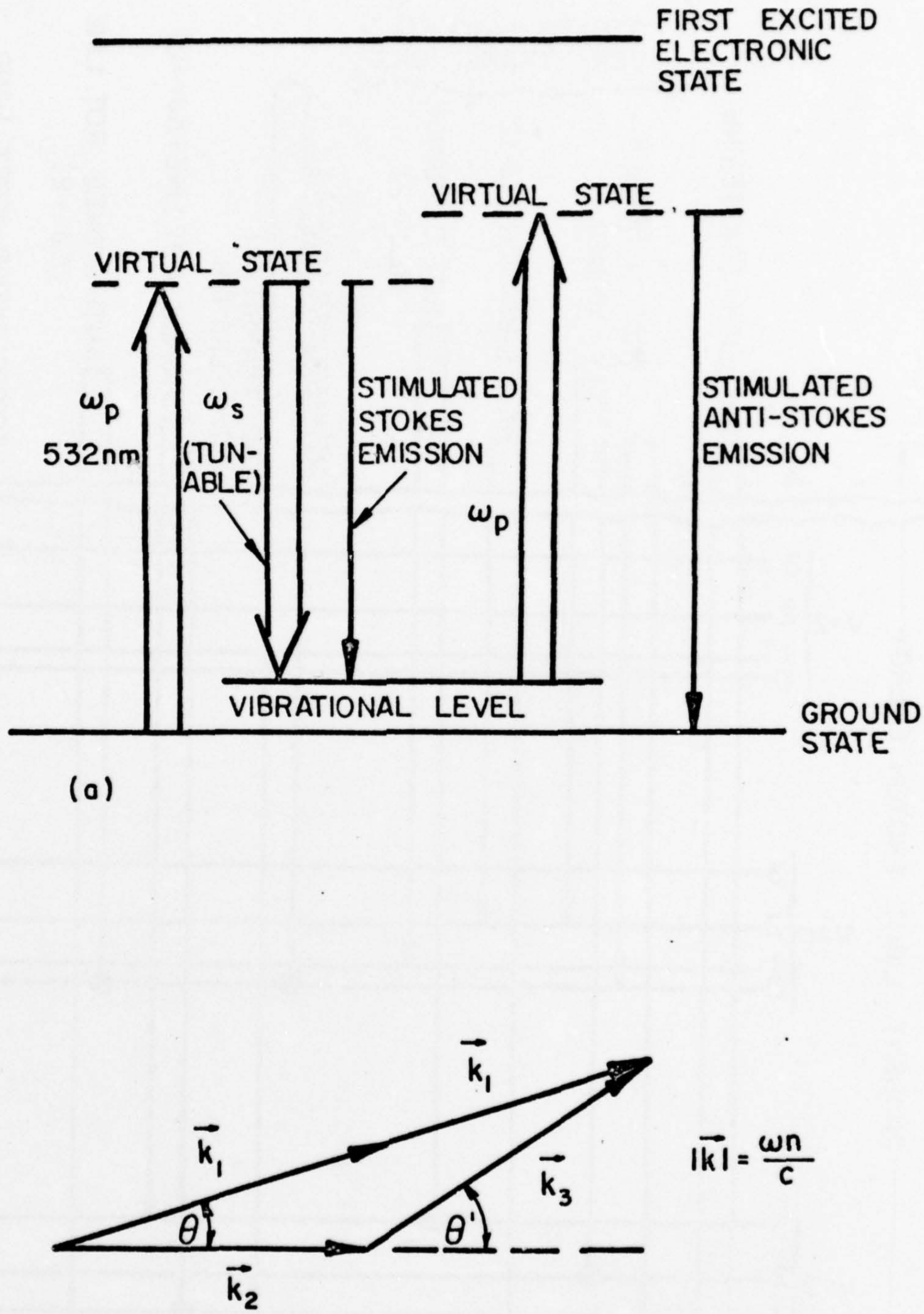

$$2\,\omega_1 - \omega_2 = \omega_3$$

$$2\,\vec{k}_1 = \vec{k}_2 + \vec{k}_3$$

FIG. 2 ENERGY LEVEL AND PHASE MATCHING DIAGRAM (REF. 11)

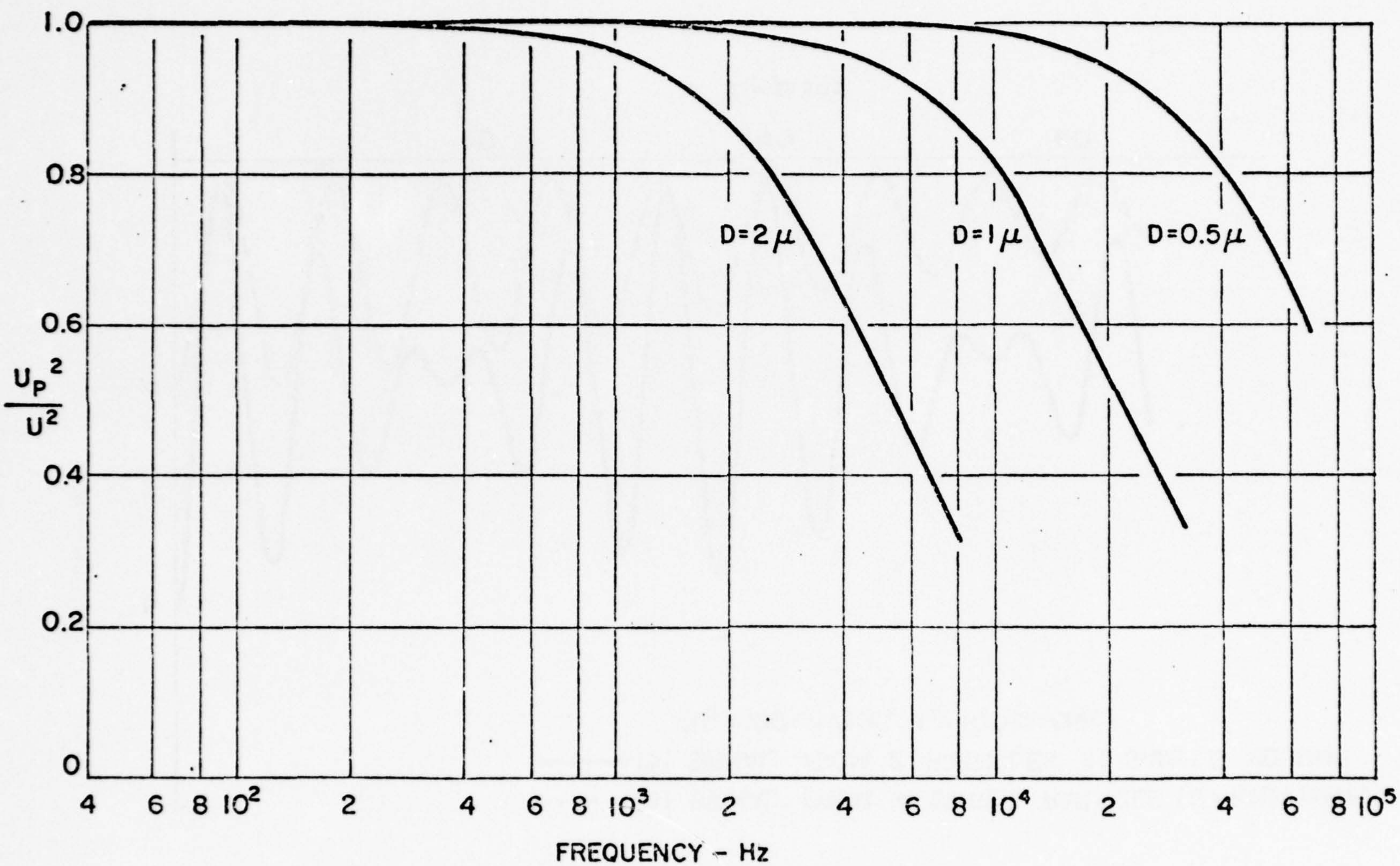

FIG. 3 RESPONSE OF ALUMINUM OXIDE PARTICLES TO TURBULENT FLUCTUATIONS

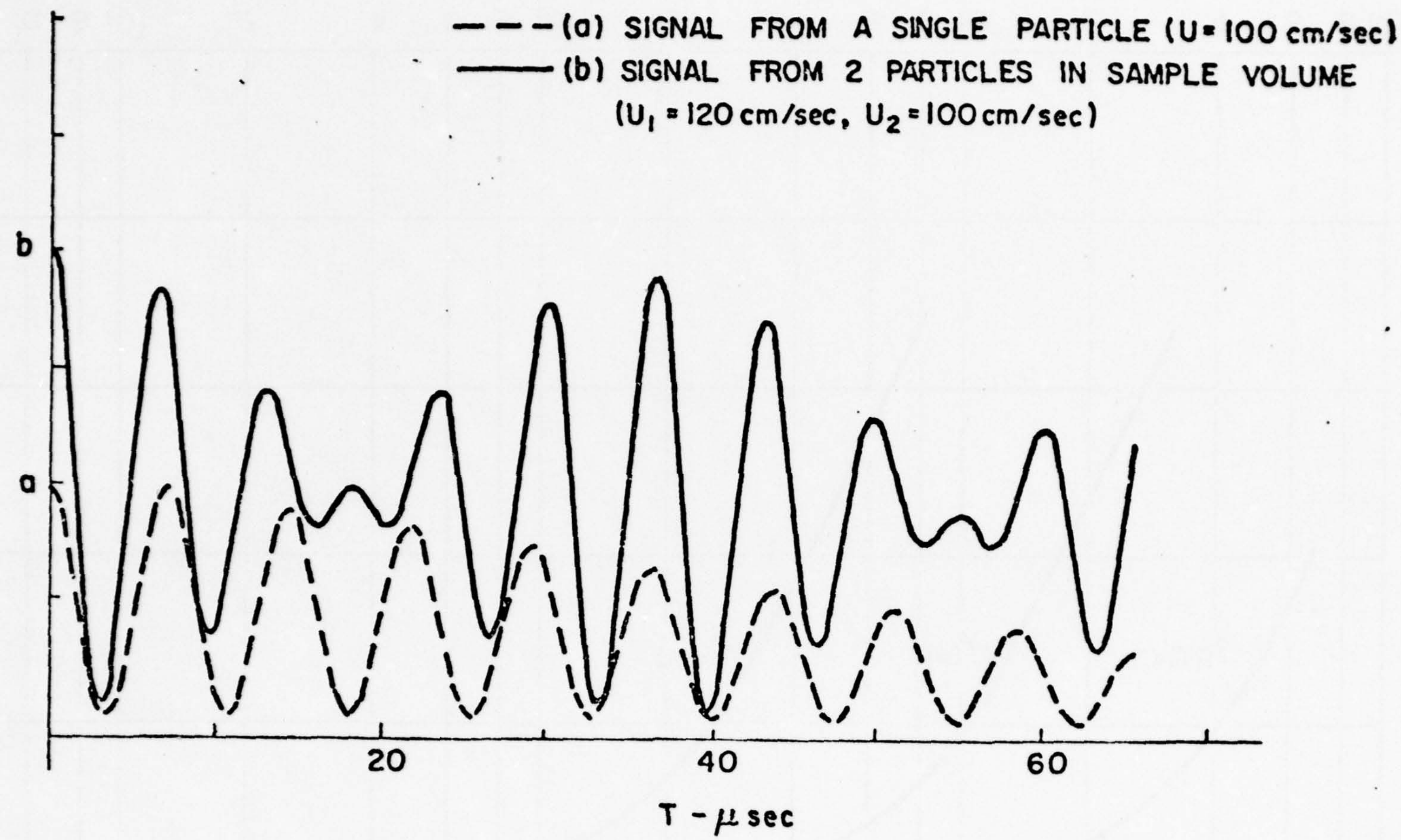

FIG. 4 COMPUTER SIMULATION OF LDV SIGNAL

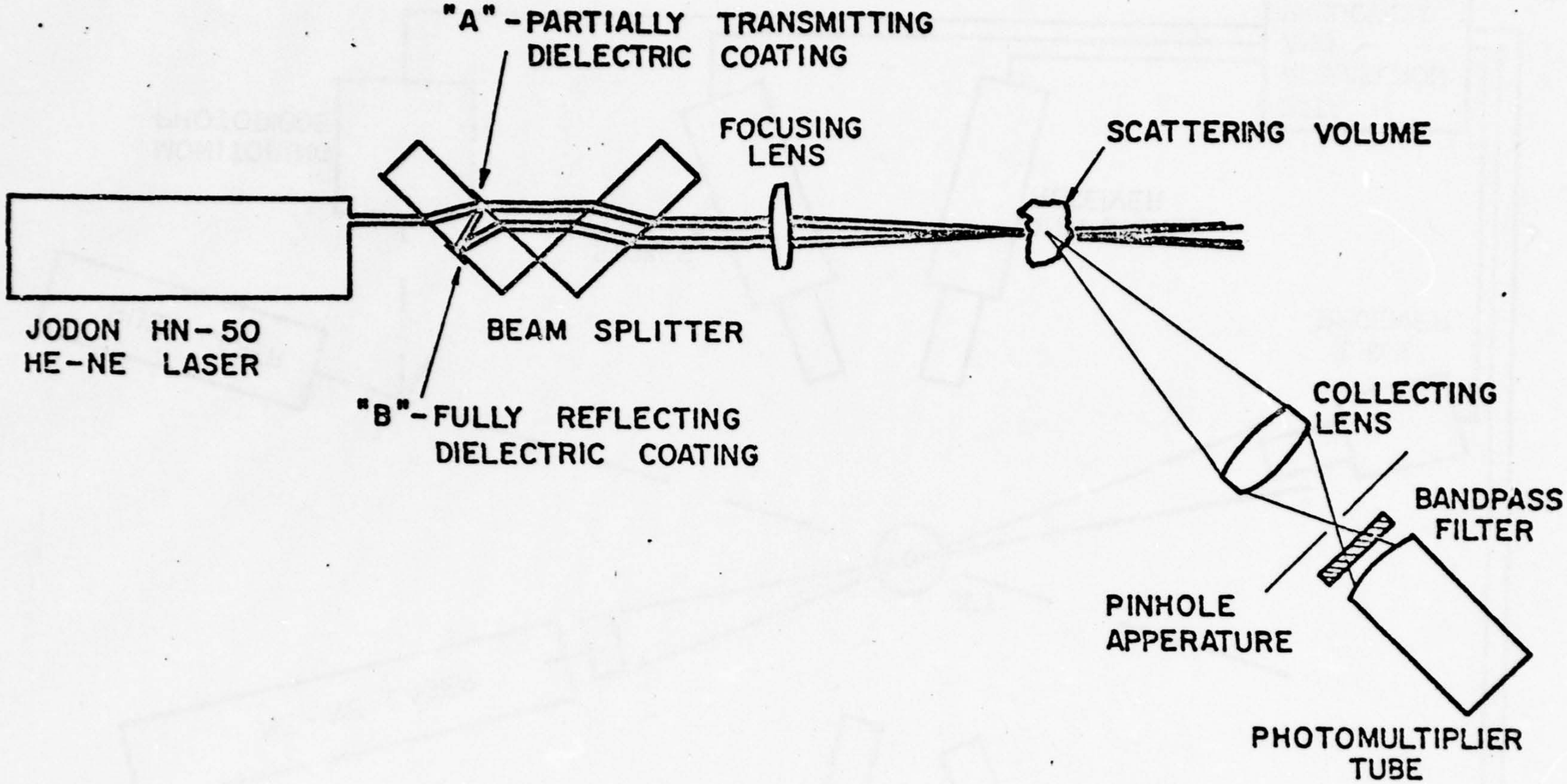

FIG. 5 SCHEMATIC DIAGRAM OF THE DUAL SCATTERER LDV SYSTEM

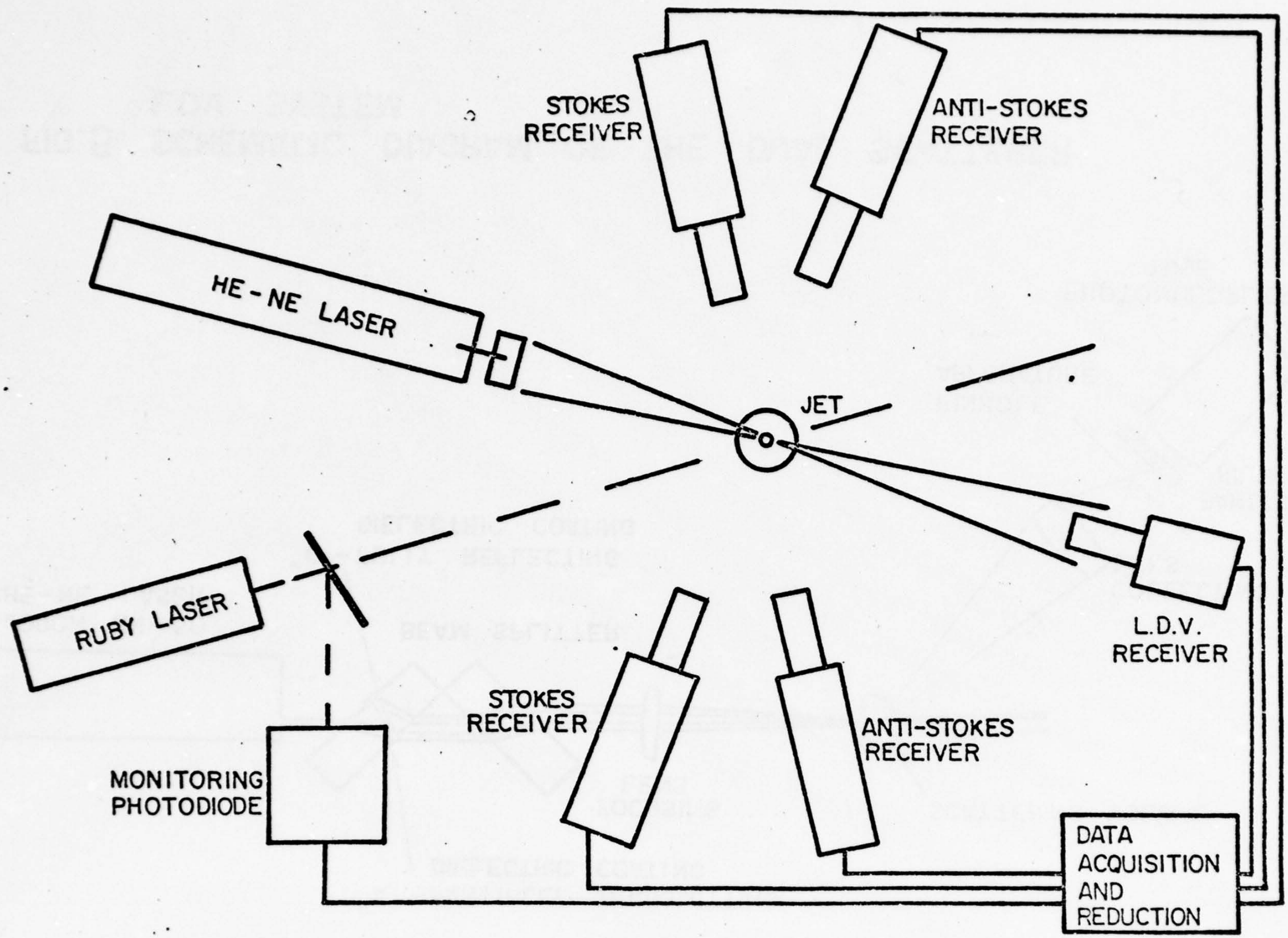

FIG. 6 BLOCK DIAGRAM OF EXPERIMENTAL APPARATUS

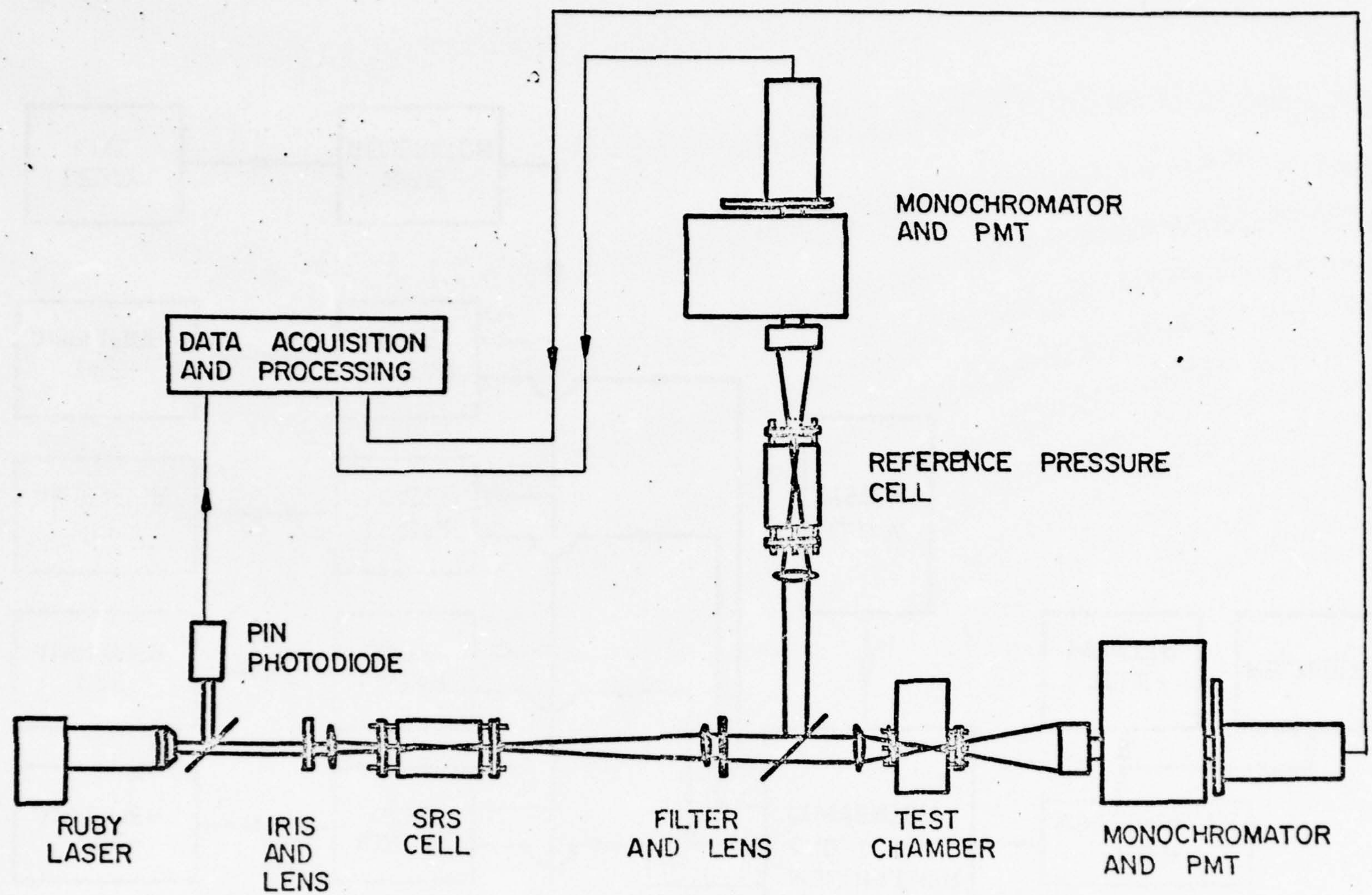

FIG. 7 SCHEMATIC DIAGRAM OF THE COHERENT RAMAN ANTI-STOKES SCATTERING APPARATUS

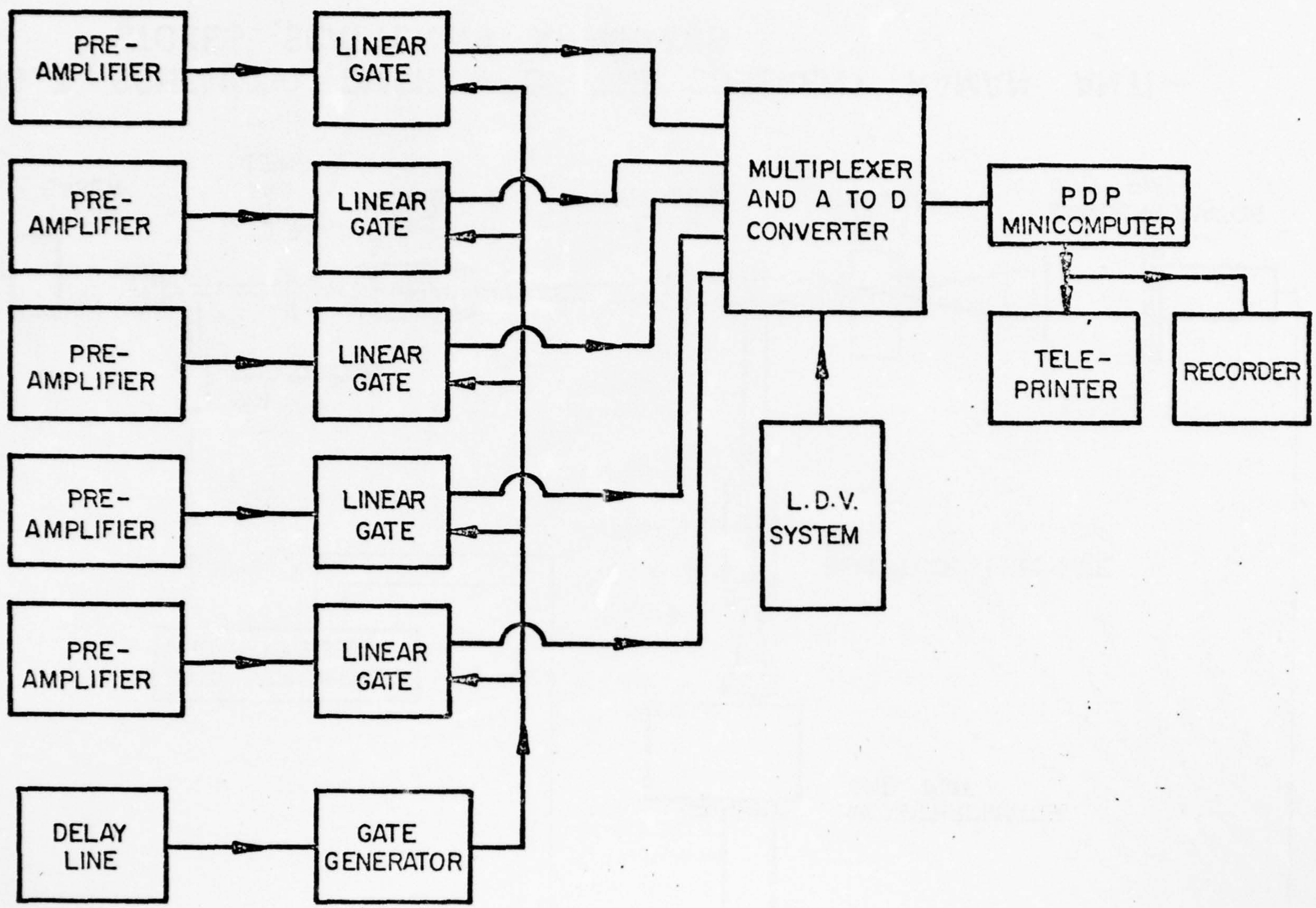

FIG. 8 DATA ACQUISITION SYSTEM

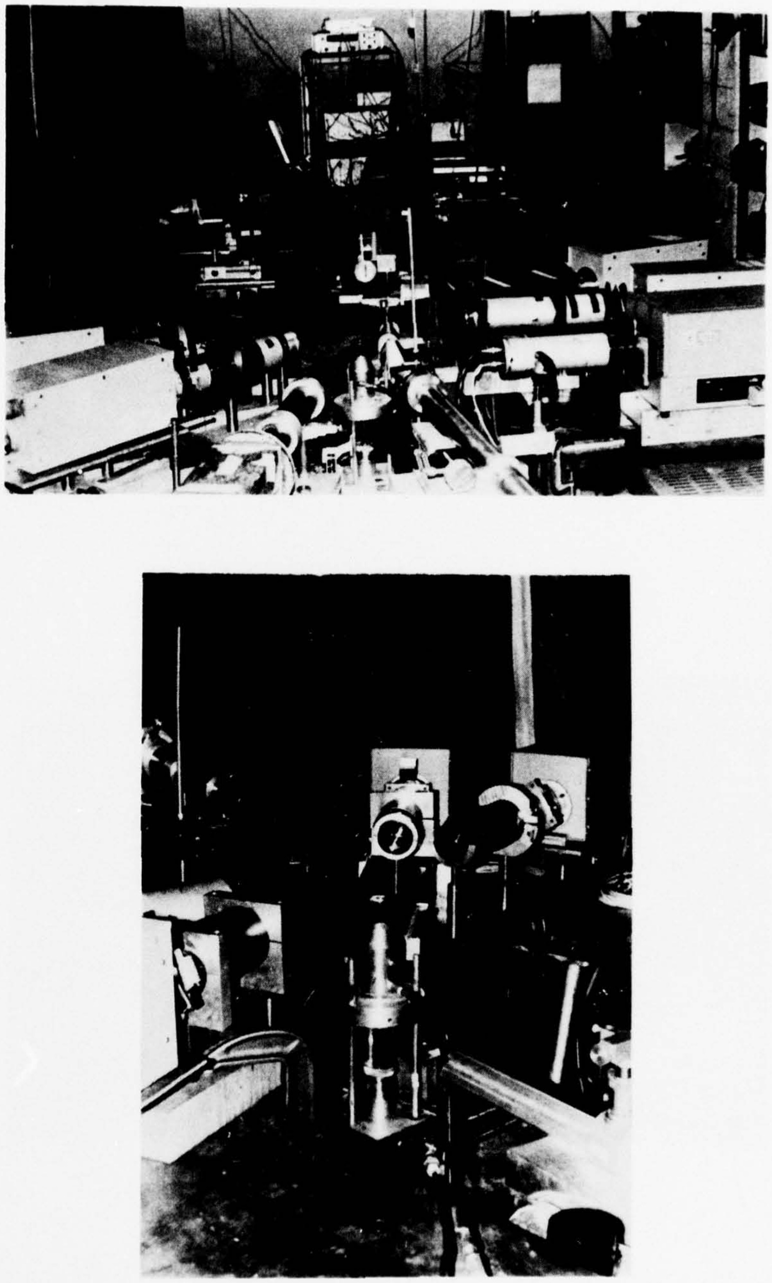

FIG. 9 PHOTOGRAPHIC VIEW OF RAMAN AND LDV APPARATUS

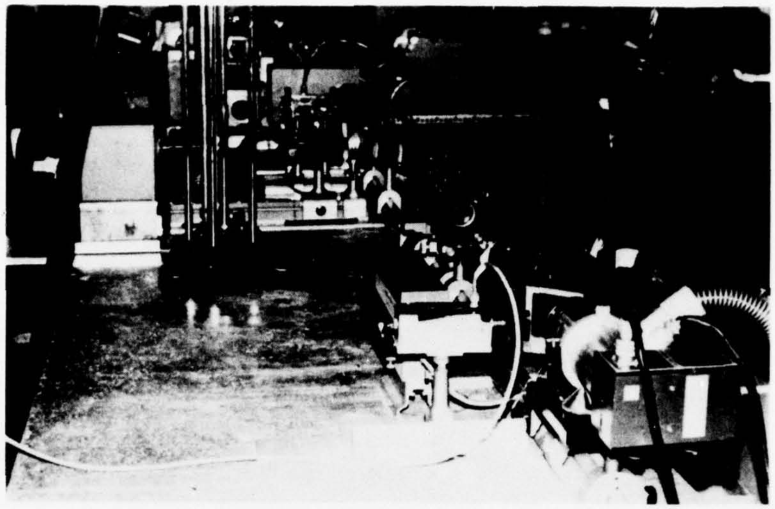

FIG. 10 PHOTOGRAPHIC VIEW OF COHERENT ANTI-STOKES SCATTERING APPARATUS

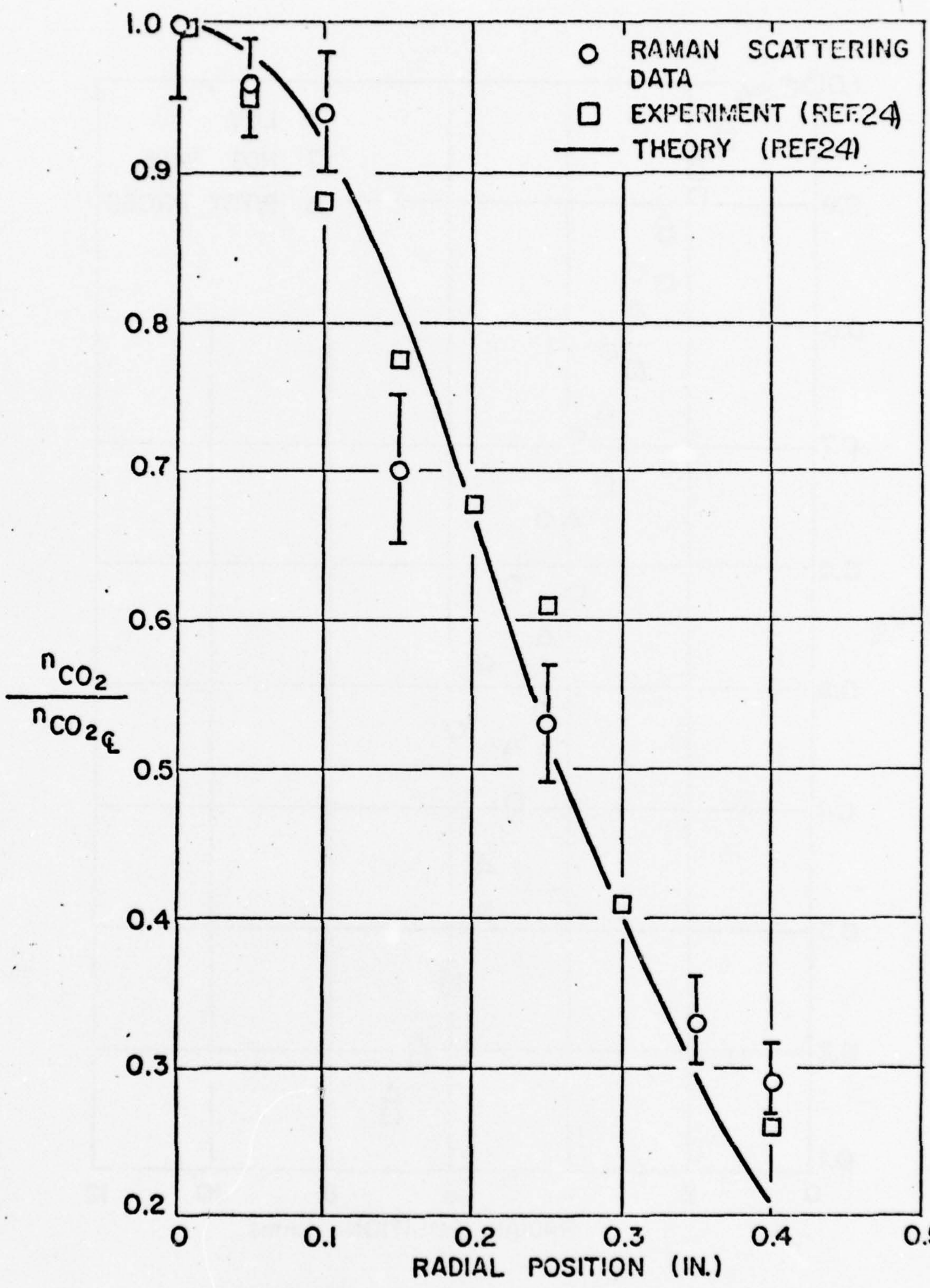

FIG. 11 SPECIE CONCENTRATION (CO_2) – AXISYMMETRIC JET

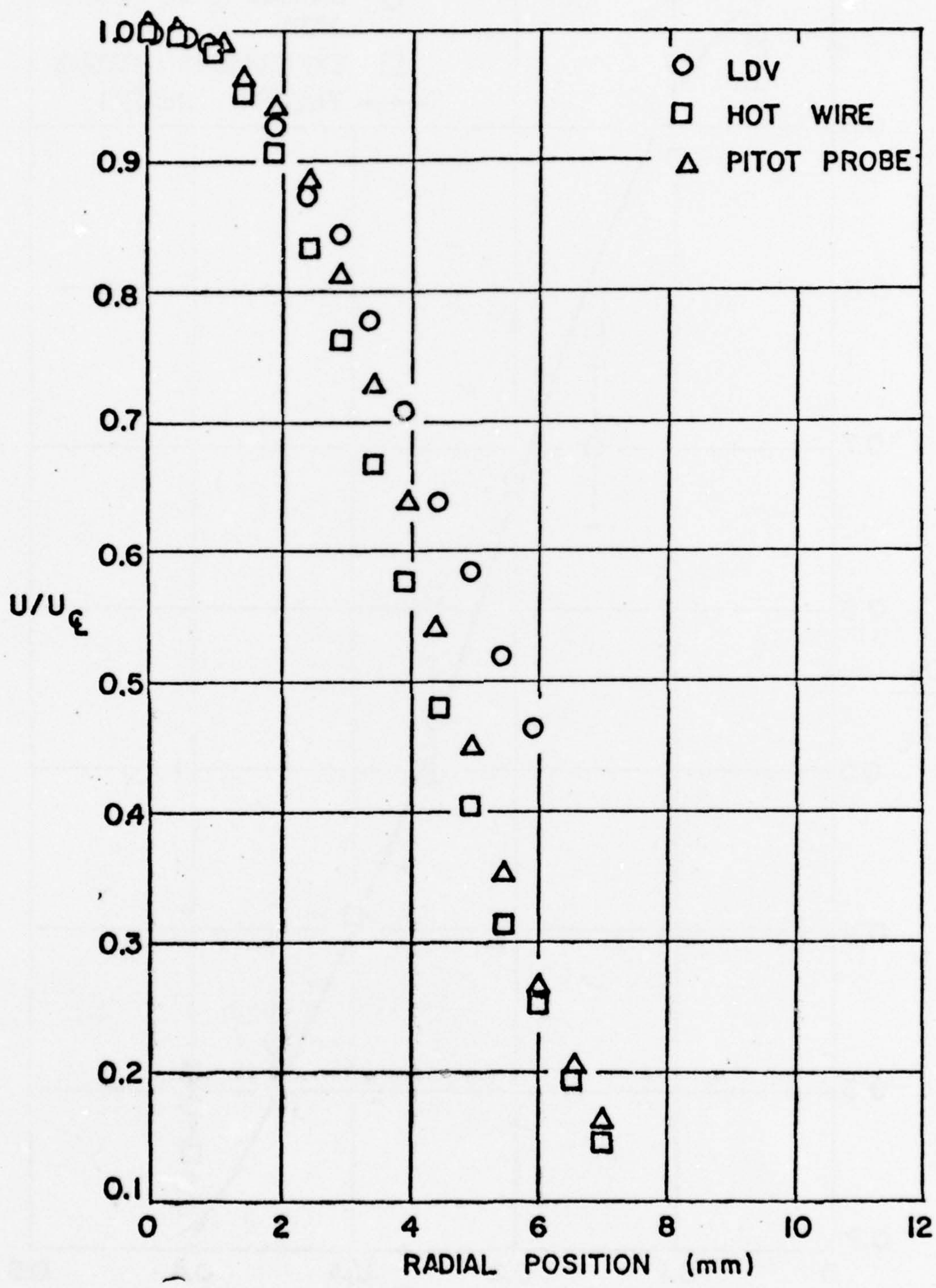

FIG. 12 COMPARISON OF VELOCITY MEASUREMENTS FOR A TURBULENT JET USING VARIOUS MEASUREMENT TECHNIQUES

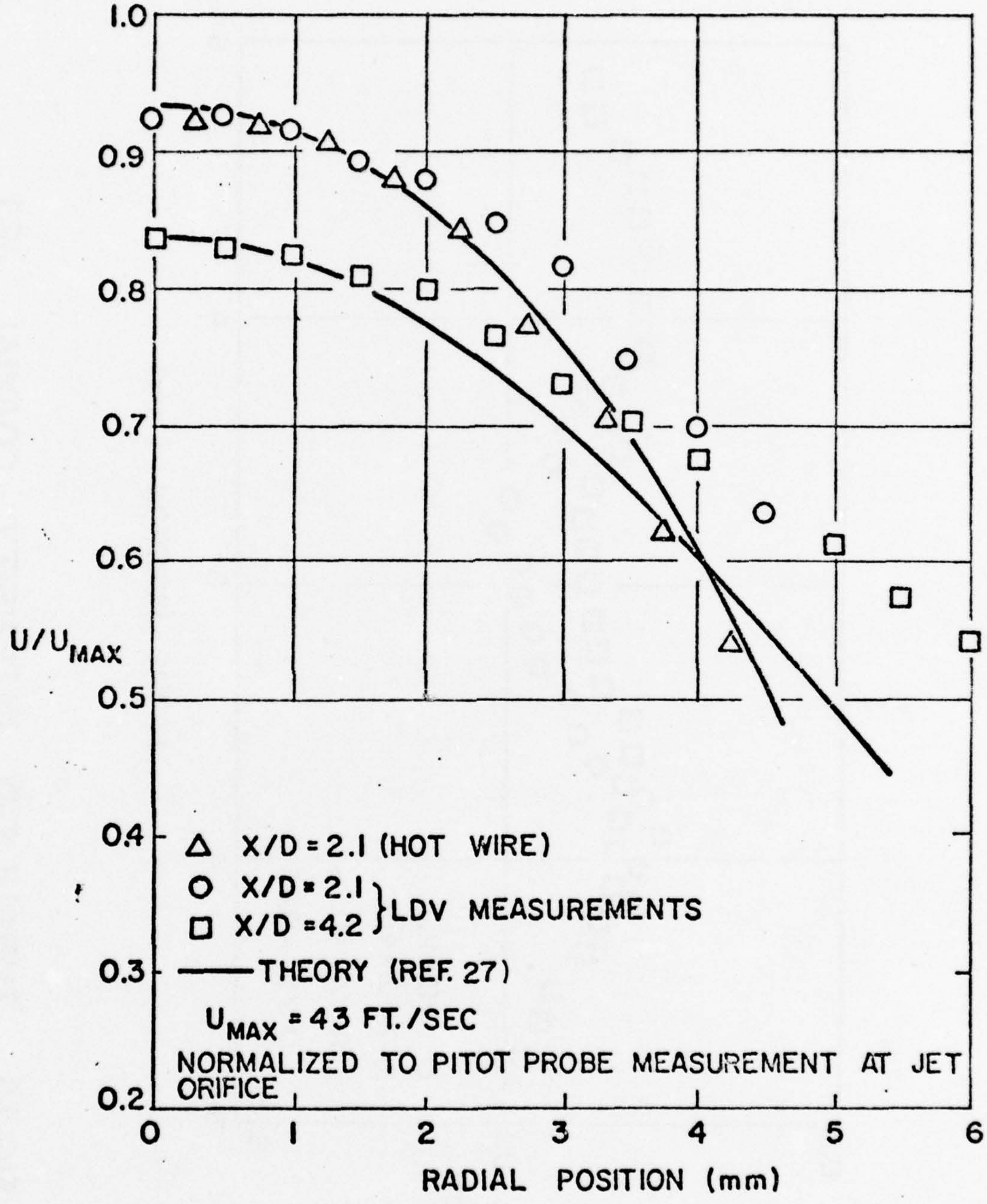

FIG. 13 RADIAL DISTRIBUTION OF $\bar{U}$ FOR COAXIAL JET — $A_o/A_i = 0.26$, $U_o/U_i = 0.45$

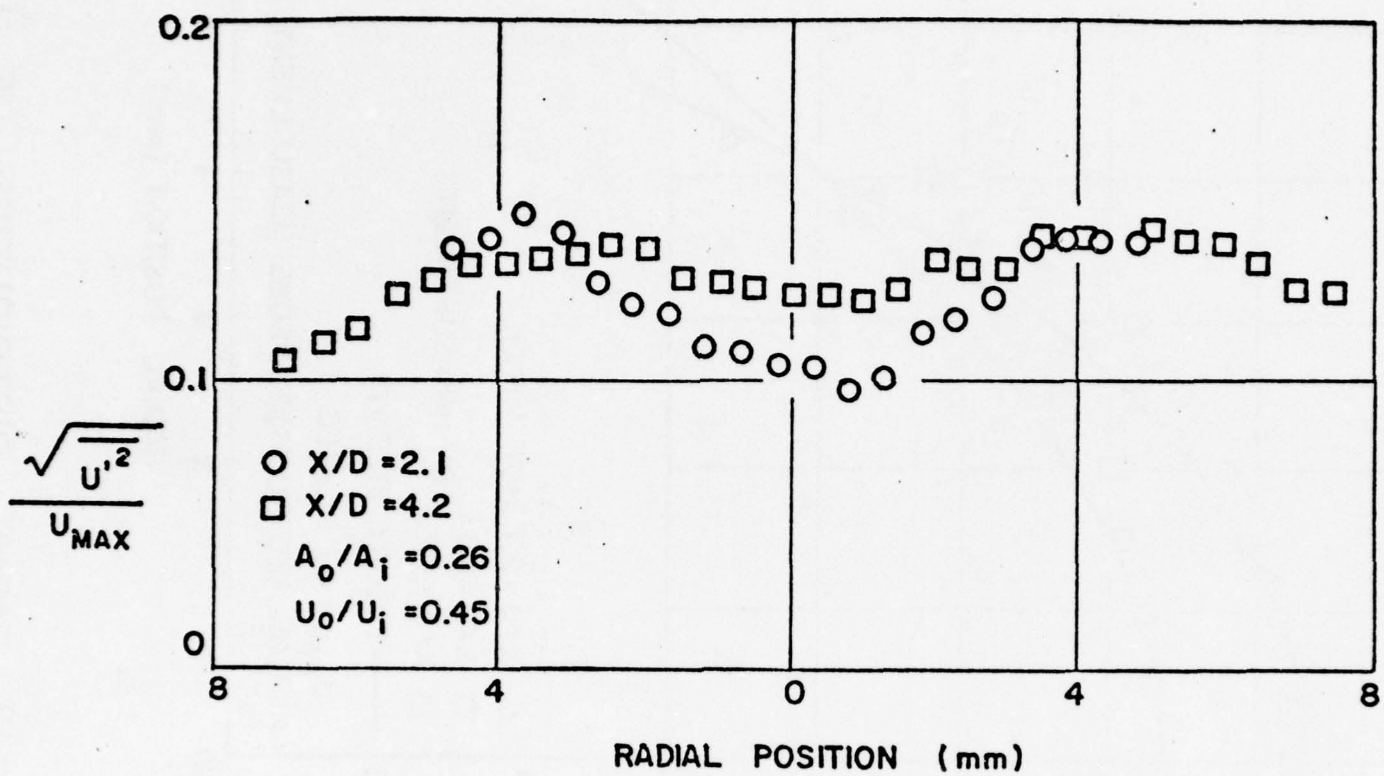

FIG. 14 TURBULENT INTENSITY - COAXIAL JET

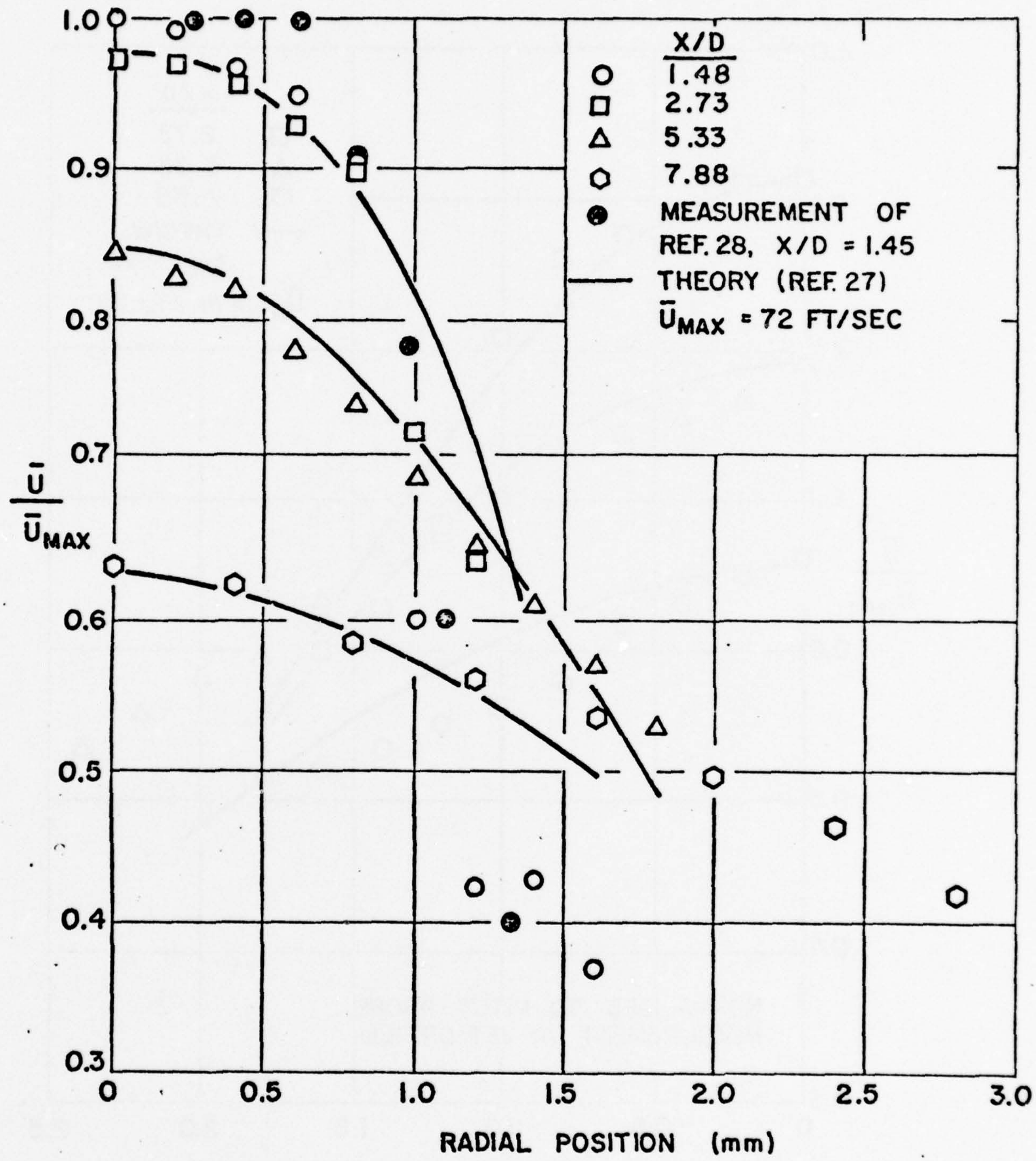

FIG. 15 RADIAL DISTRIBUTION OF $\bar{U}$ – $U_o/U_i = 0.5$, $A_o/A_i = 1.28$

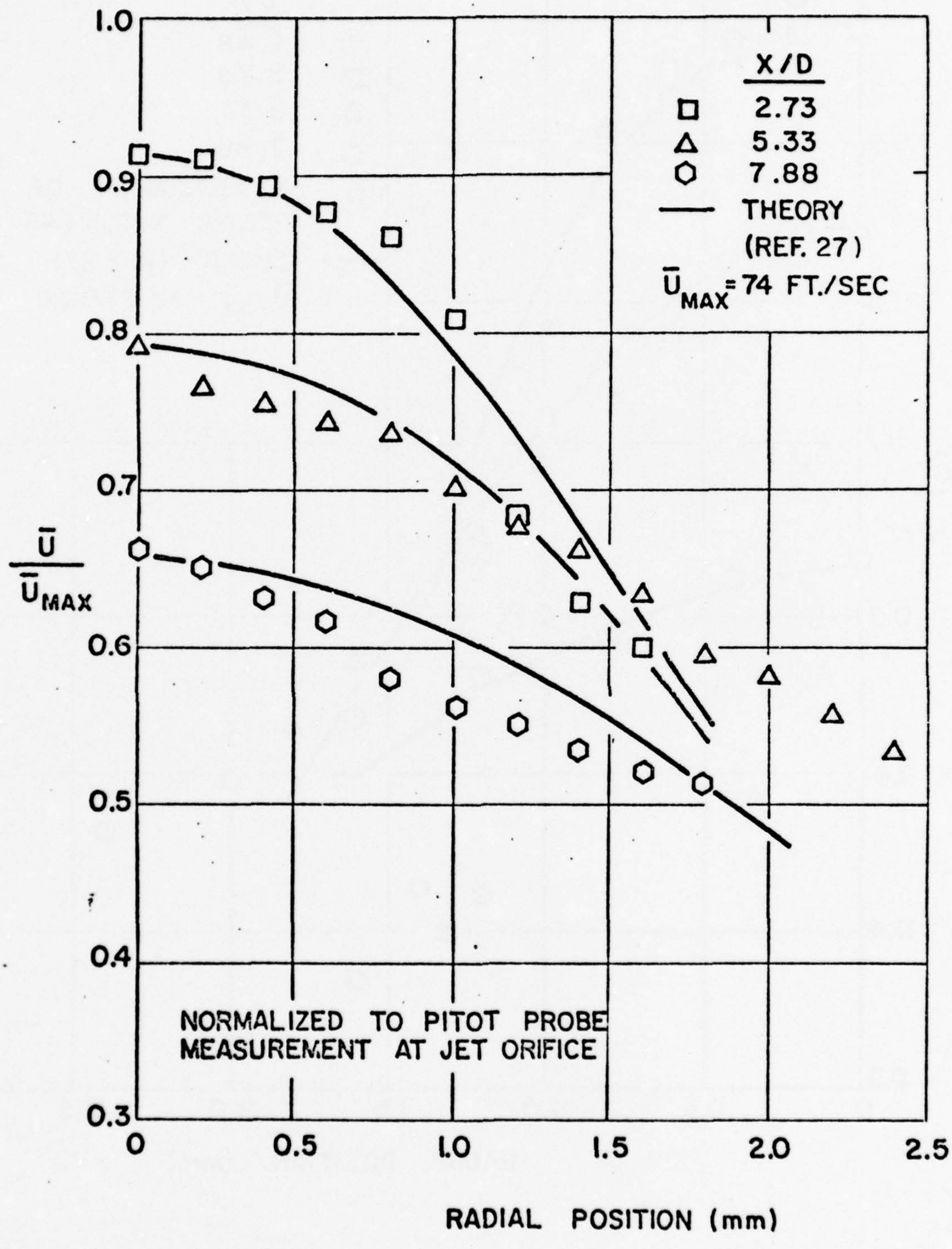

FIG. 16 RADIAL DISTRIBUTION OF $\bar{U}$ - U_o/U_i=0.74, A_o/A_i=1.28

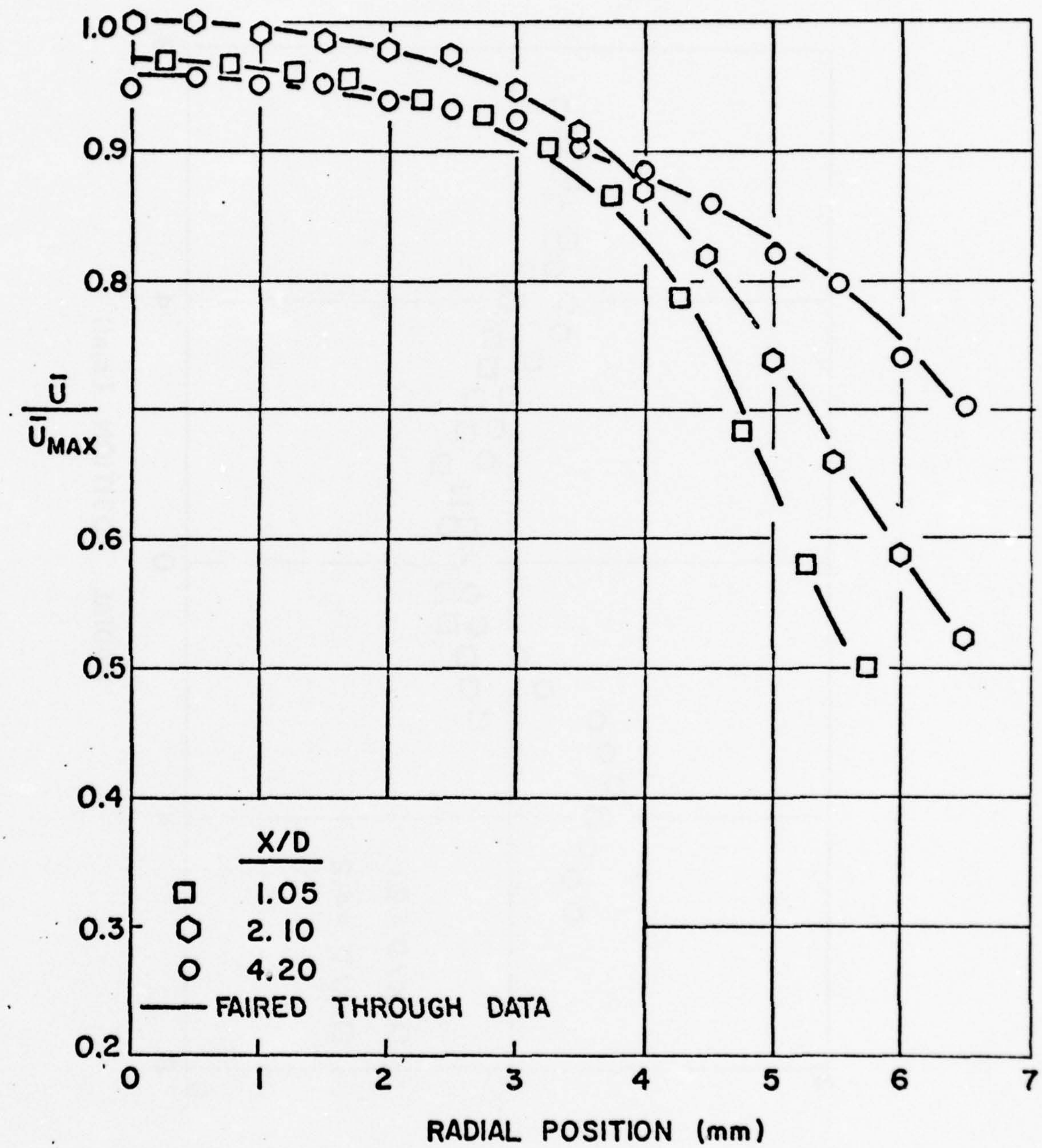

FIG. 17 RADIAL DISTRIBUTION OF $\bar{U}$ - METHANE-AIR FLAME

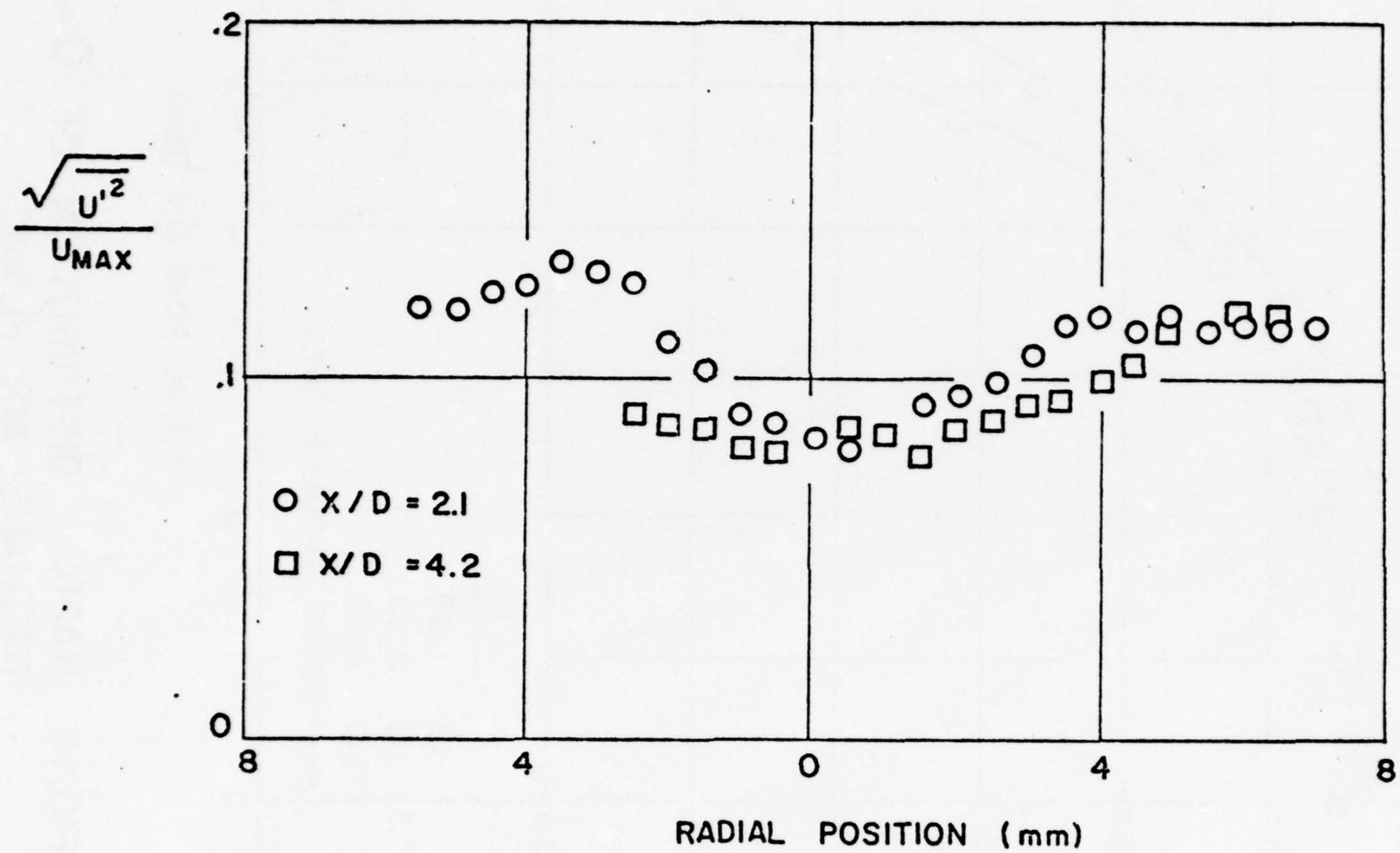

FIG. 18 TURBULENT INTENSITY IN A FLAME

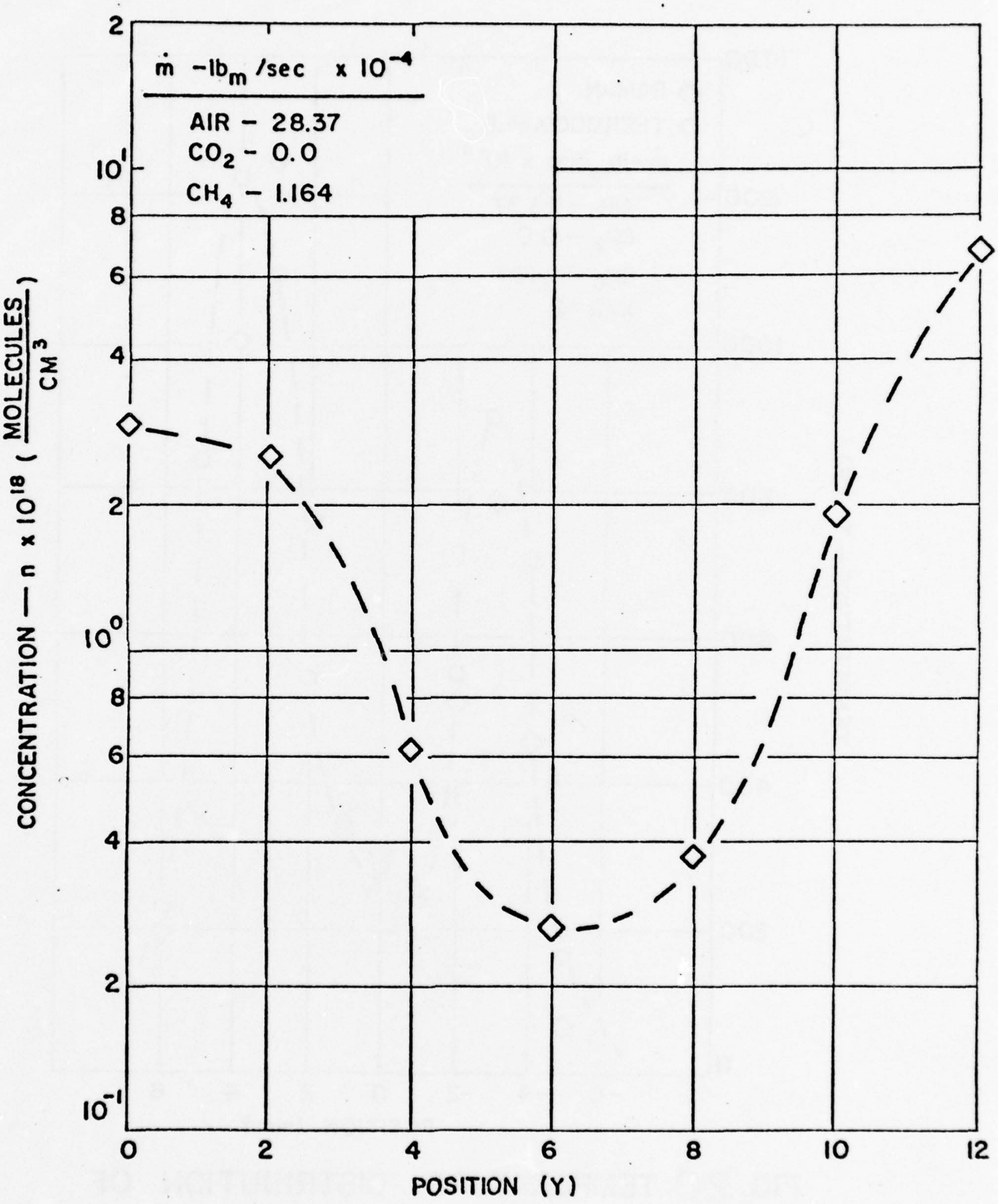

FIG. 19 VARIATION OF N_2 CONCENTRATION WITH POSITION AT X/D = 2

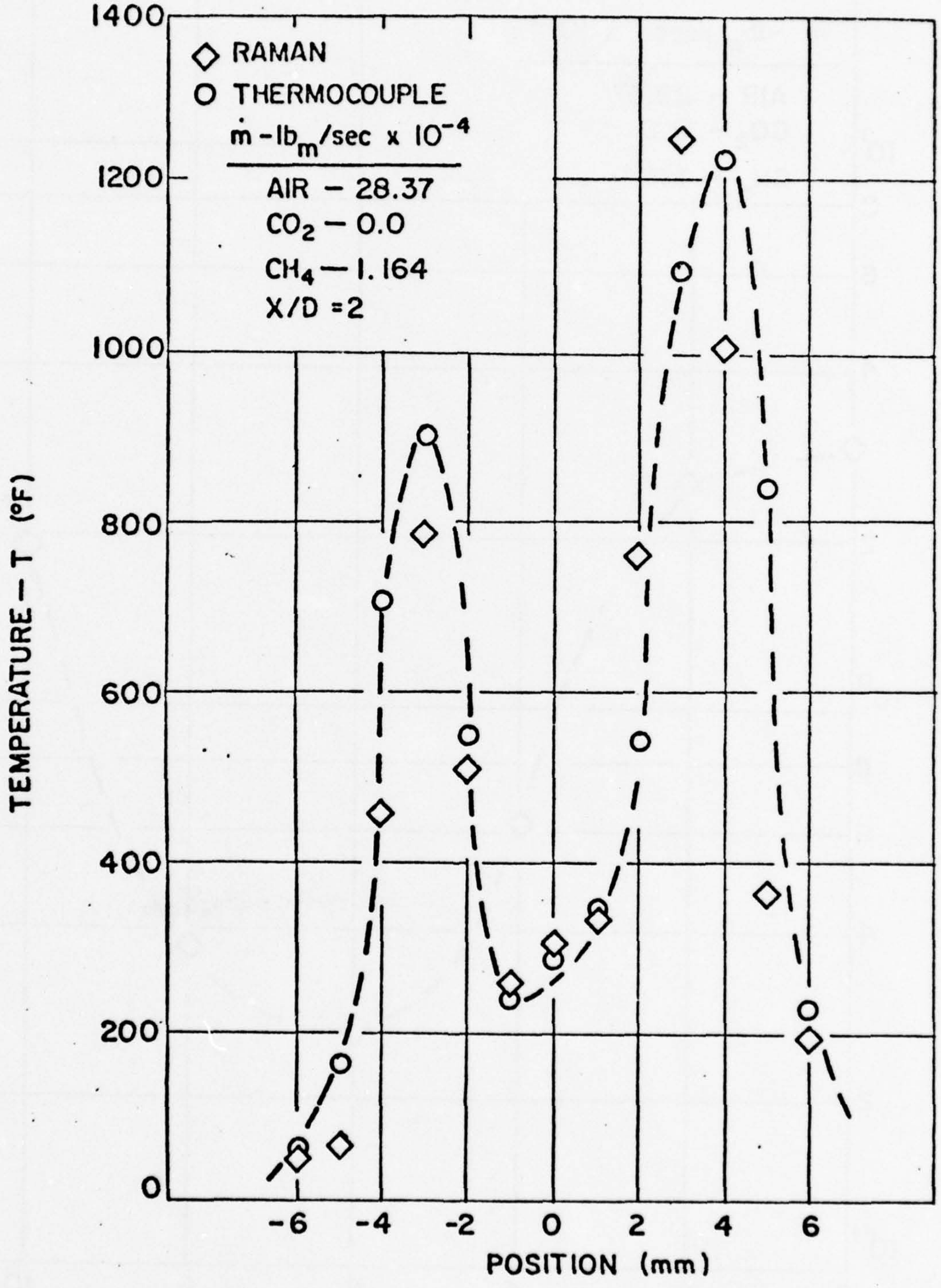

FIG. 20 TEMPERATURE DISTRIBUTION OF FLAME MONITORING N_2

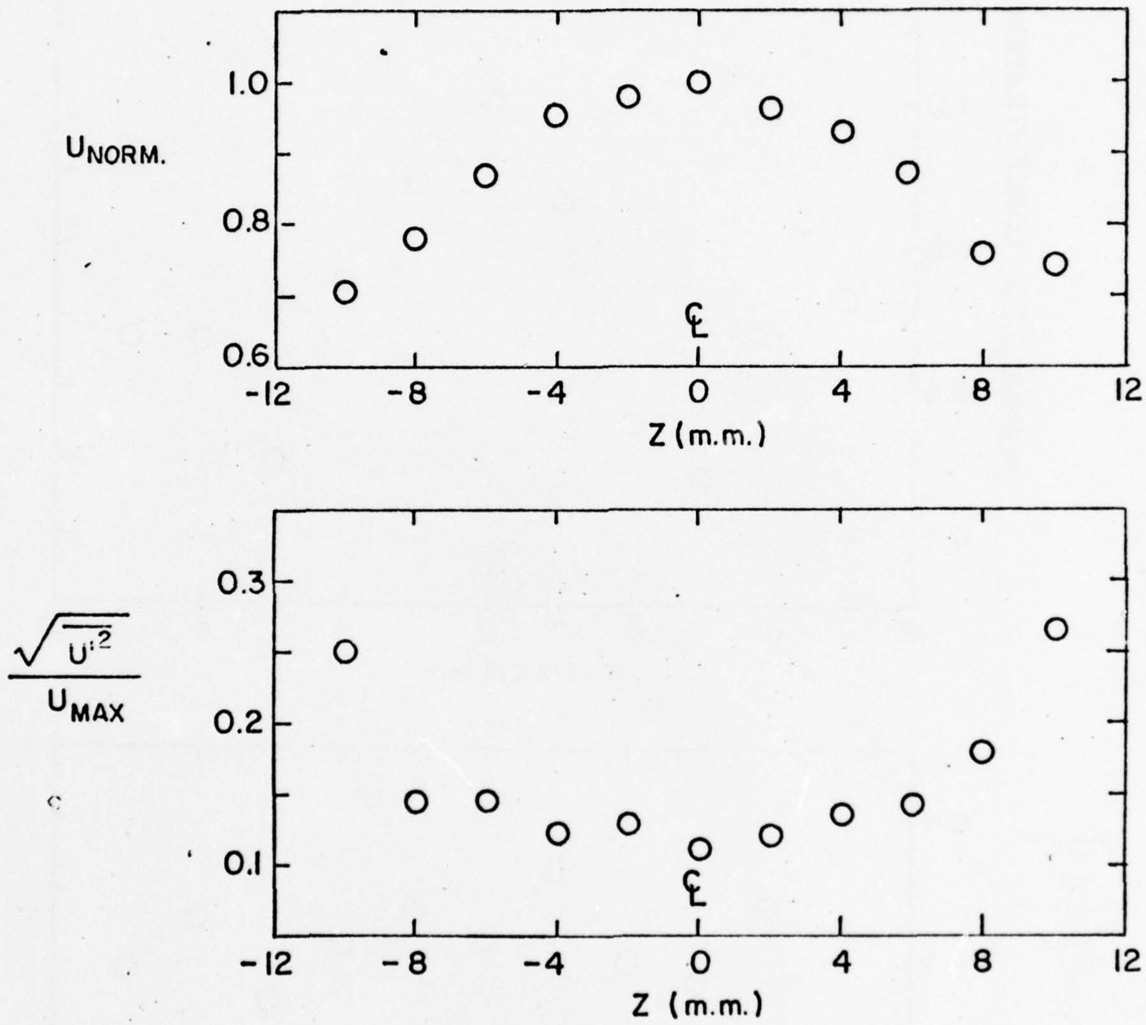

FIG.21 VELOCITY AND TURBULENT INTENSITY PROFILE IN A FLAME AT X/D = 5.2

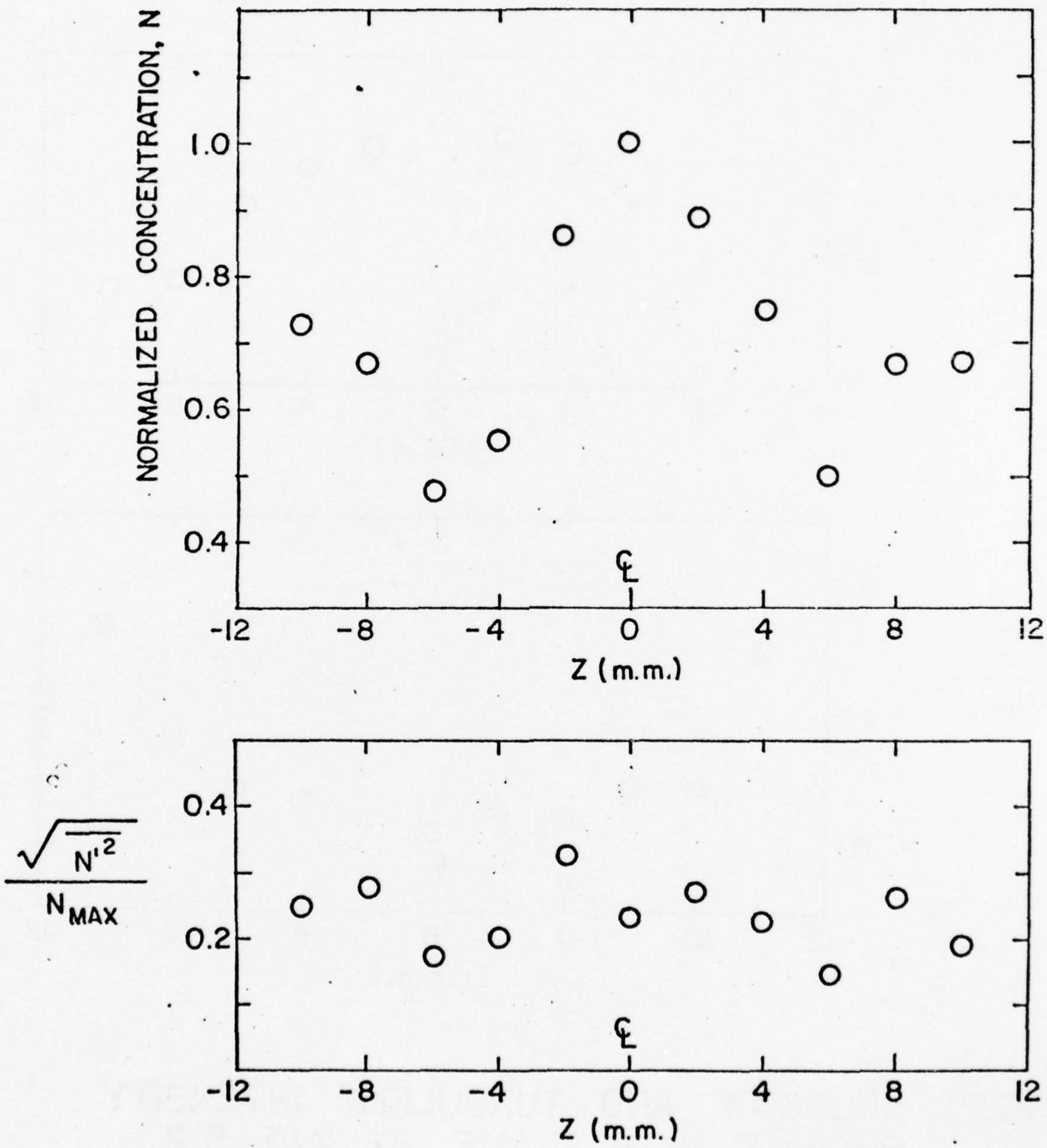

FIG. 22 NORMALIZED CONCENTRATION OF N_2 IN A FLAME AT X/D = 5.2 AND THE CONCENTRATION FLUCTUATION

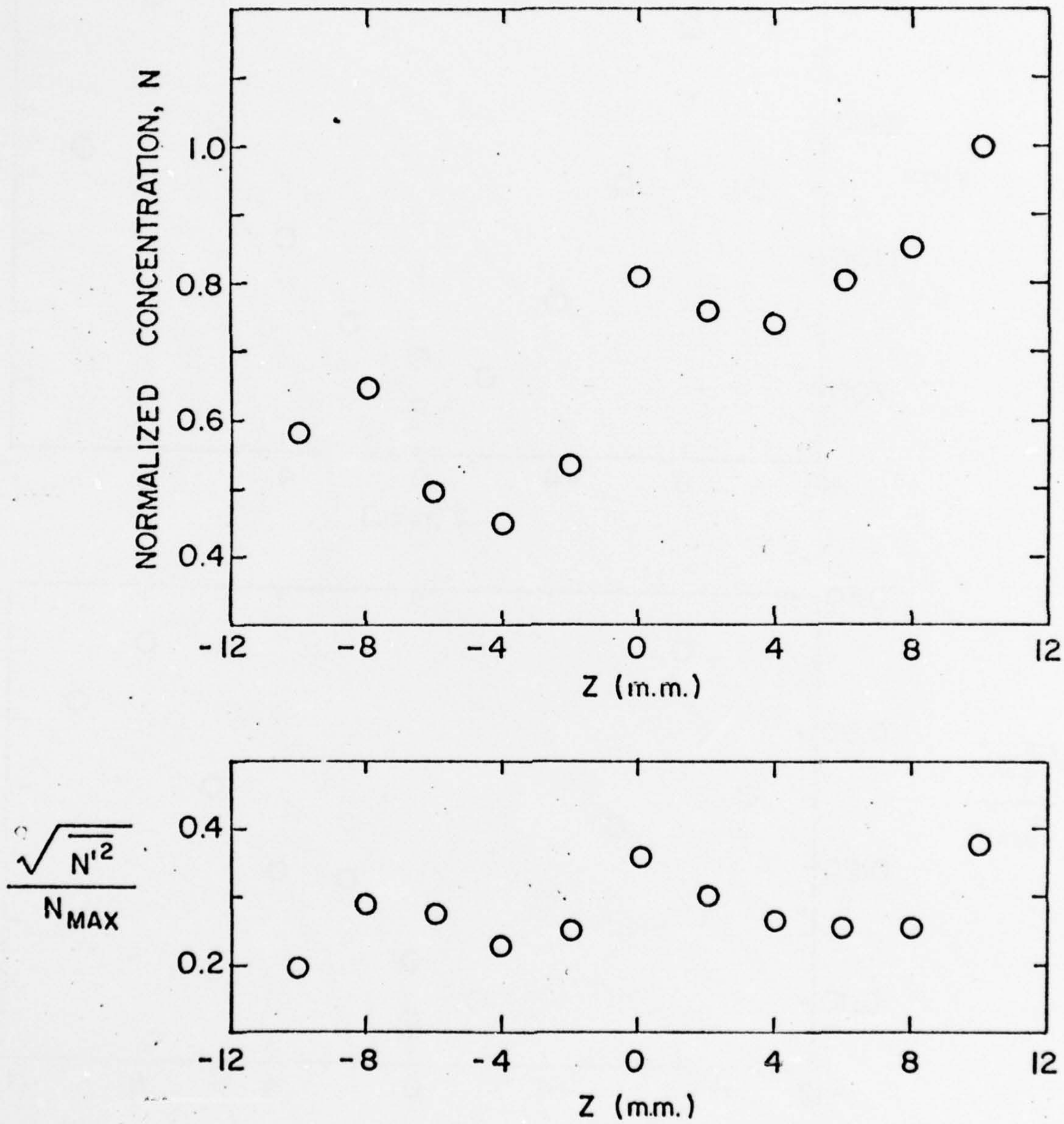

FIG. 23 NORMALIZED CONCENTRATION OF CO_2 IN A FLAME AT X/D =5.2 AND THE CONCENTRATION FLUCTUATION

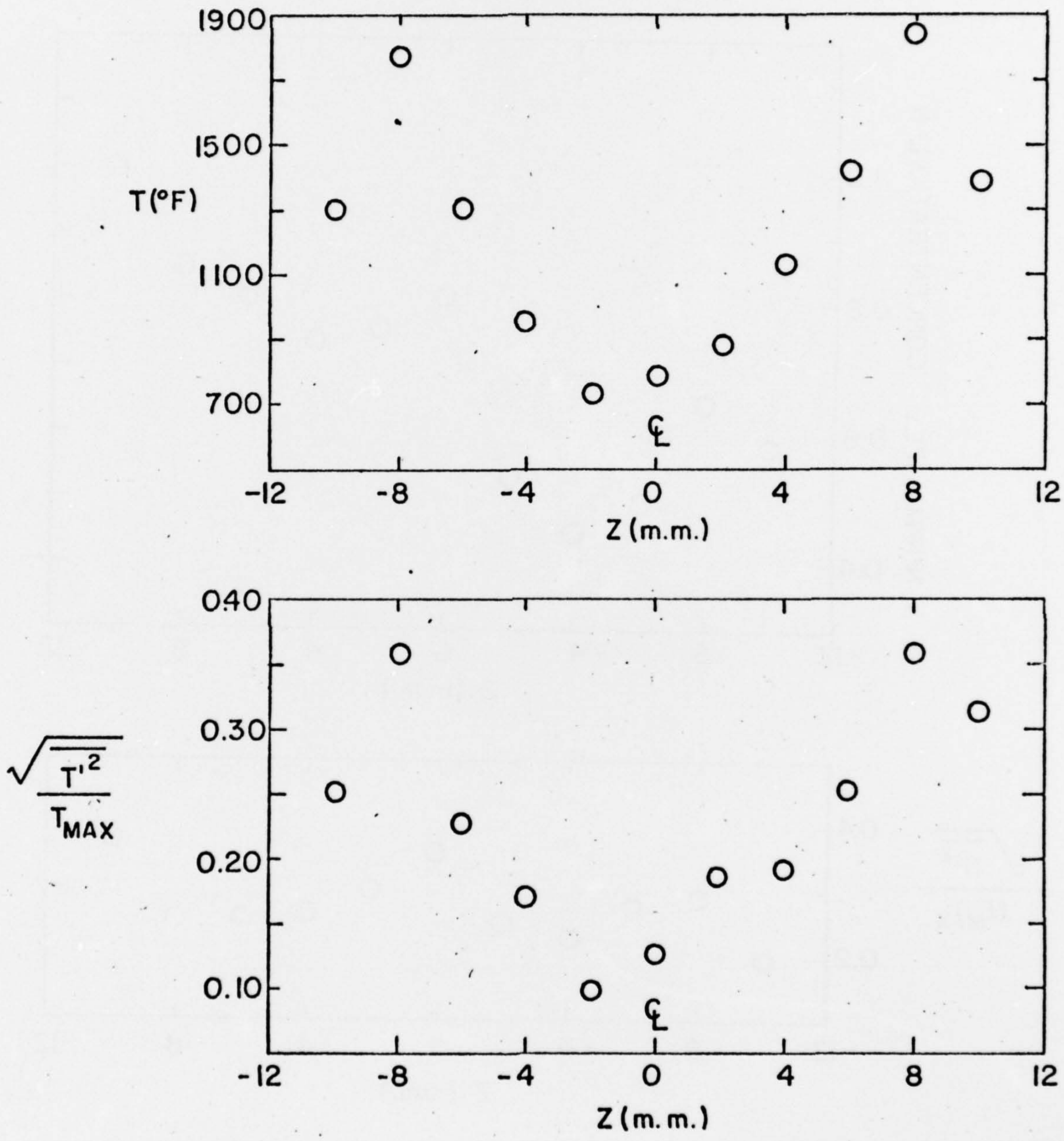

FIG.24 TEMPERATURE AND TEMPERATURE FLUCTUATION PROFILE IN A FLAME AT X/D = 5.2 (N_2)

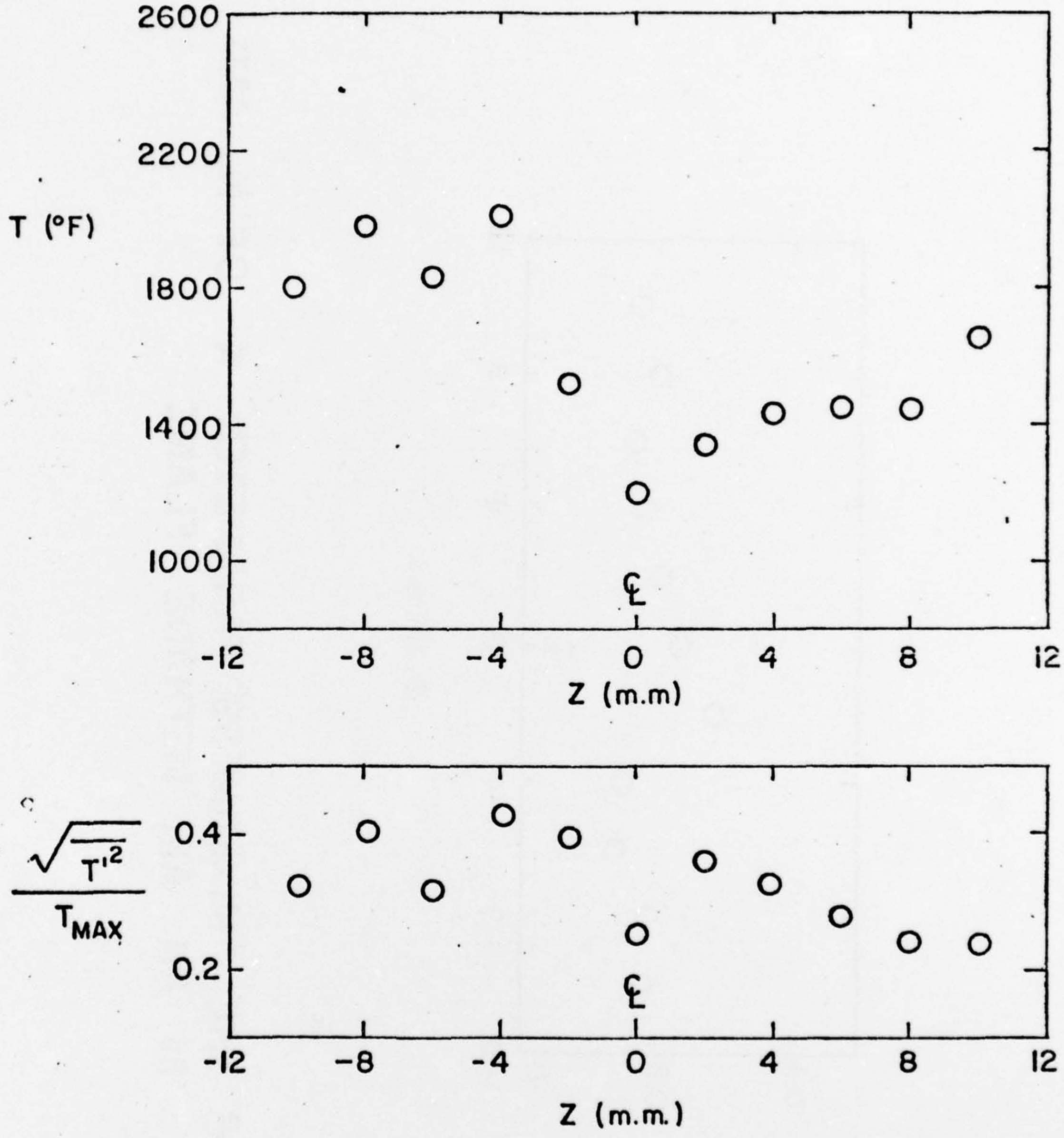

FIG.25 TEMPERATURE AND TEMPERATURE FLUCTUATION OF CO_2 IN A FLAME AT X/D = 5.2

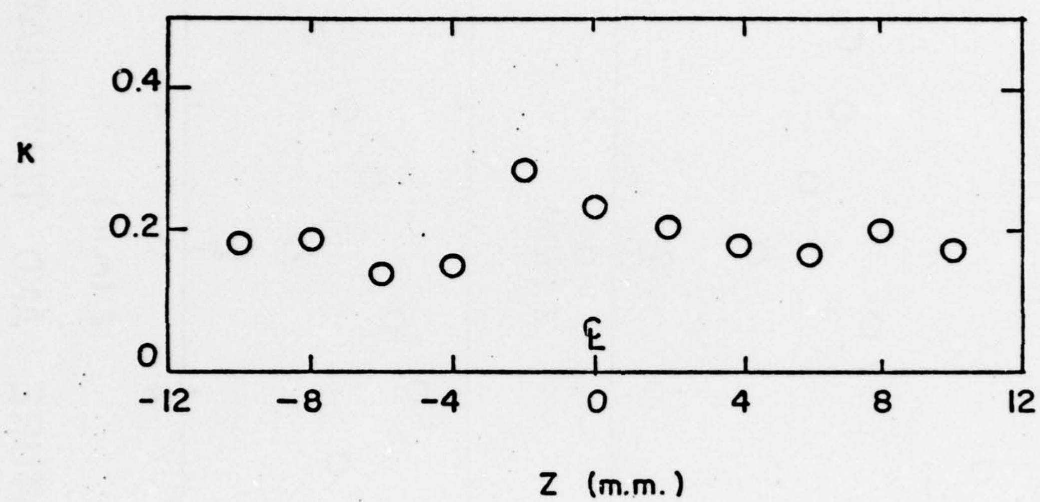

FIG.26 THE "MIXEDNESS" PARAMETER K OF N_2 AND CO_2 IN AN AIR METHANE FLAME

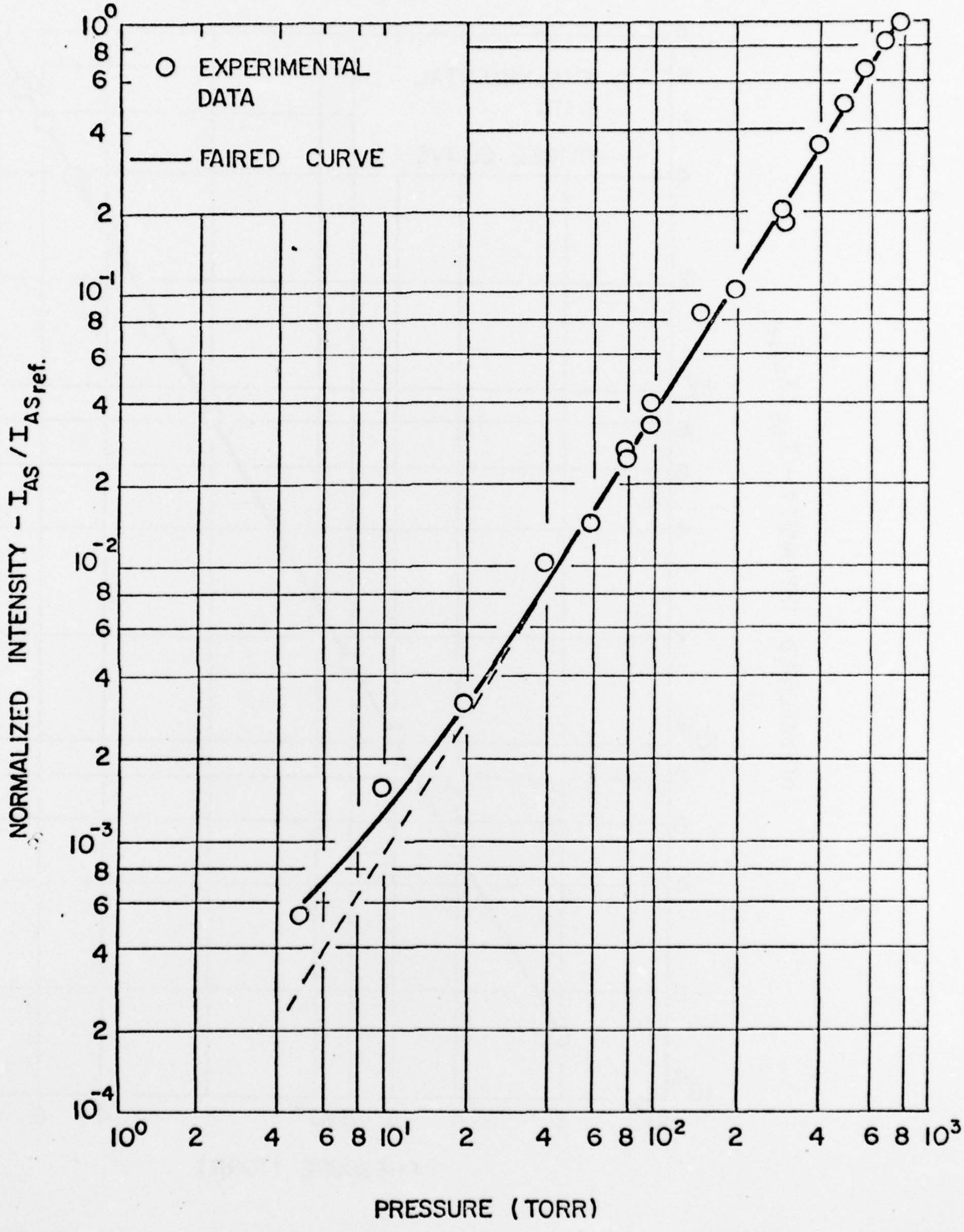

FIG.27 MEASURED COHERENT RAMAN ANTI-STOKES INTENSITY OF METHANE (CH_4) AS A FUNCTION OF PRESSURE

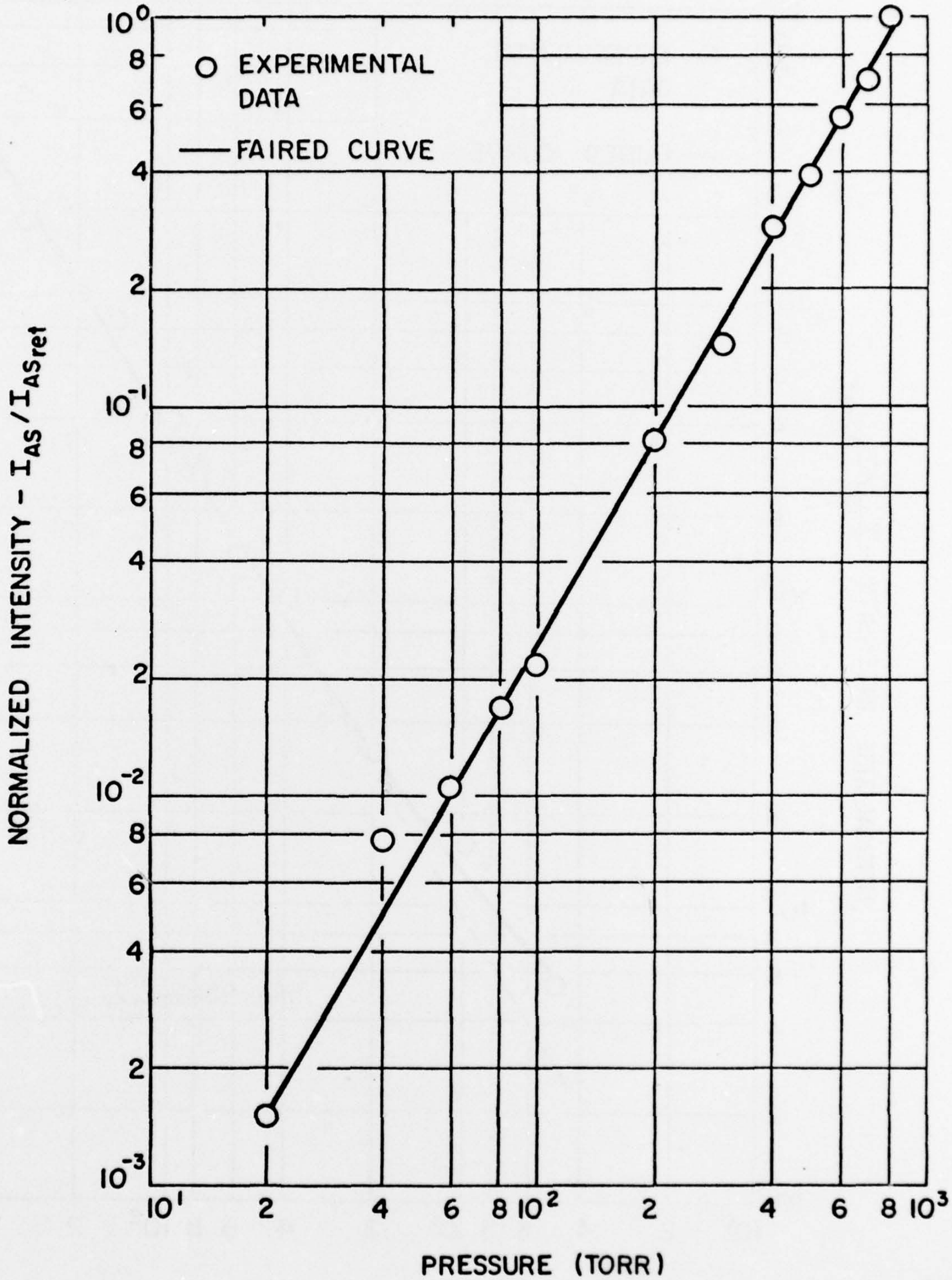

FIG. 28 MEASURED COHERENT RAMAN ANTI-STOKES INTENSITY OF HYDROGEN (H_2) AS A FUNCTION OF PRESSURE

GOVERNMENT AGENCIES

1. British Embassy
   3100 Massachusetts Avenue, N.W.
   Washington, D.C. 20008
   ATTN: Mr. J. Barry Jamieson
   Propulsion Officer

2. Central Intelligence Agency
   Washington, D.C. 20505
   ATTN: CRS/ADD/Publications

3. Institute for Defense Analyses
   400 Army-Navy Drive
   Arlington, Virginia 22202
   ATTN: Dr. Hans G. Wolfhard,
   Sen. Staff

4. Defense Documentation Center
   Cameron Station
   Alexandria, Virginia 22314

5. EPA Technical Center
   Research Triangle Park
   North Carolina 27711
   ATTN: Dr. W. Herget, P-222

6. Esso Research and Engineering Company
   Government Research Laboratory
   P.O. Box 8
   Linden, New Jersey 07036
   ATTN: Dr. William F. Taylor

7. Arnold Air Force Station
   Tennessee 36389
   ATTN: AEDC (DYF)

8. Arnold Air Force Station
   Tennessee 37389
   ATTN: R.E. Smith, Jr., Chief
   T-Cells Division
   Engine Test Facility

9. Air Force Aero Propulsion Laboratory
   Wright-Patterson Air Force Base
   Ohio 45433
   ATTN: STINFO Office

10. Air Force Eastern Test Range
    MU-135
    Patrick Air Force Base
    Florida 32925
    ATTN: AFETR Technical Library

11. Air Force Office of Scientific Research
    Bolling Air Force Base, Building 410
    Washington, D.C. 20332
    ATTN: Dr. Joseph F. Masi

12. Air Force Aero Propulsion Laboratory
    Wright-Patterson AFB, Ohio 45433
    ATTN: AFAPL/TBC
    Dr. Kervyn Mach

13. Air Force Aero Propulsion Laboratory
    Wright-Patterson AFB, Ohio 45433
    ATTN: AFAPL/TBC
    Francis R. Ostdiek

14. Air Force Rocket Propulsion Laboratory
    Department of Defense
    Edwards AFB, California 93523
    ATTN: LKCG (Mr. Selph)

15. U.S. Army Air Mobility Research and
    Development Laboratory
    Eustis Directorate
    Fort Eustis, Virginia 23604
    ATTN: Propulsion Division
    (SAVDL-EU-PP)

16. U.S. Army Artillery Combat
    Developments Agency
    Fort Sill, Oklahoma 73503
    ATTN: Commanding Officer

17. U.S. Army Missile Command
    Redstone Arsenal, Alabama 35809
    ATTN: AMSMI-RR

18. U.S. Army Missile Command
    Redstone Scientific Information Center
    Redstone Arsenal, Alabama 35809
    ATTN: Chief, Document Section

19. Indiana State Library
    140 North Senate Avenue
    Indianapolis, Indiana 46204
    ATTN: Patricia Matkovic
    Reference Librarian
    % Indiana Division

20. NASA Headquarters
    600 Independence
    Washington, D.C. 20546
    ATTN: Dr. Gordon Banerian

21. NASA Headquarters
    Aeronautical Propulsion Division
    Code RL, Deputy Director
    Office of Advanced Research & Technology
    Washington, D.C. 20546
    ATTN: Mr. Nelson F. Rekos

22. NASA Ames Research Center
    Deputy Chief Aeronautics Division
    Mail Stop 27-4
    Moffett Field, California 94035
    ATTN: Mr. Edward W. Perkins

23. NASA Ames Research Center
    Aerodynamics Branch 227-8
    Moffett Field, California 94305
    ATTN: Mr. Ira R. Schwartz

24. NASA Lewis Research Center
    21000 Brookpark Road
    Cleveland, Ohio 44135
    ATTN: D. Morris, Mail Stop 60-3

25. NASA Lewis Research Center
    Hypersonic Propulsion Section
    Mail Stop 6-1
    21000 Brookpark Road
    Cleveland, Ohio 44135
    ATTN: Dr. Louis A. Povinelli

26. NASA Marshall Space Flight Center
    S&E ASTN-P
    Huntsville, Alabama 35812
    ATTN: Mr. Keith Chandler

27. National Science Foundation
    Engineering Energetics
    Engineering Division
    Washington, D.C. 20550
    ATTN: Dr. George Lee

28. National Science Foundation
    Engineering Energetics
    Engineering Division
    Washington, D.C. 20550
    ATTN: Dr. M. Ojalvo

29. National Science Foundation
    Engineering Energetics
    Engineering Division
    Washington, D.C. 20550
    ATTN: Dr. Royal Rostenbach

30. Naval Air Development Center
    Commanding Officer (AD-5)
    Warminster, Pennsylvania 18974
    ATTN: NADC Library

31. Naval Air Propulsion Test Center (R&T)
    Trenton, New Jersey 08628
    ATTN: Mr. Al Martino

32. Naval Air Systems Command
Department of the Navy
Washington, D.C. 20360
ATTN: Research Administrator
AIR 310

33. Naval Air Systems Command
Department of the Navy
Washington, D.C. 20360
ATTN: Propulsion Technology Admin.
AIR 330

34. Naval Air Systems Command
Department of the Navy
Washington, D.C. 20360
ATTN: Technical Library Division
AIR 604

35. Naval Ammunition Depot
Research and Development Department
Building 190
Crane, Indiana 47522
ATTN: Mr. B.E. Douda

36. Naval Ordnance Laboratory Commander
White Oak
Silver Springs, Maryland 20910
ATTN: Library

37. Naval Ordnance Systems Command
Department of the Navy
Washington, D.C. 20360
ATTN: ORD 0331

38. Naval Postgraduate School
Department of Aeronautics, Code 57
Monterey, California 93940
ATTN: Dr. Allen E. Fuhs

39. Naval Postgraduate School
Library (Code 2124)
Monetrey, California 93940
ATTN: Superintendent

40. Naval Postgraduate School
Monterey, California 93940
ATTN: Library (Code 0212)

41. Office of Naval Research Branch Office
1030 East Green Street
Pasadena, California 91106
ATTN: Dr. Rudolph J. Marcus

42. Office of Naval Research Branch Office
536 South Clark Street
Chicago, Illinois 60605
ATTN: Commander

43. Office of Naval Research Branch Office
495 Summer Street
Boston, Massachusetts 02210
ATTN: Commander

44. Office of Naval Research
Power Branch, Code 473
Department of the Navy
Arlington, Virginia 22217

45. Office of Naval Research
Fluid Dynamics Branch, Code 438
Department of the Navy
Washington, D.C. 22217
ATTN: Mr. Morton Cooper

46. Naval Research Lab
Code 7710
Washington, D.C. 20390
ATTN: W.W. Balwanz

47. Naval Research Laboratory Director
Washington, D.C. 20390
ATTN: Technical Information Division

48. Naval Research Laboratory Director
Washington, D.C. 20390
ATTN: Library Code 2629 (ONRL)

49. Naval Ship Research and Development Center
Annapolis Division
Annapolis, Maryland 21402
ATTN: Library, Code A214

50. Naval Ship Systems Command
Department of the Navy
Washington, D.C. 20360
ATTN: Technical Library

51. Naval Weapons Center Commander
China Lake, California 93555
ATTN: Airbreathing Propulsion Branch
Code 4583

52. Naval Weapons Center
Chemistry Division
China Lake, California 93555
ATTN: Dr. William S. McEwan
Code 605

53. Naval Weapons Center
Commander
China Lake, California 93555
ATTN: Technical Library

54. Naval Weapons Center
Code 608, Thermochemistry Group
China Lake, California 93555
ATTN: Mr. Edward W. Price, Head

55. Naval Weapons Laboratory
Dahlgren, Virginia 22448
ATTN: Technical Library

56. Naval Undersea Research and
Development Center
San Diego, California 92132
ATTN: Technical Library
Code 1311D

57. Naval Underwater Systems Center
Fort Trumbull
New London, Connecticut 06320
ATTN: Technical Library

58. Naval Underwater Systems Center
Code 5B-331
Newport, Rhode Island 02840
ATTN: Dr. Robert Lazar

59. Picatinny Arsenal
Commanding Officer
Dover, New Jersey 07801
ATTN: Technical Information Library

60. State Documents Section
Exchange and Gift Division
Washington, D.C. 20540
ATTN: Library of Congress

U.S. INDUSTRIES AND LABORATORIES

61. AeroChem Research Laboratories, Inc.
P.O. Box 12
Princeton, New Jersey 08540
ATTN: Dr. Arthur Fontijn

62. AeroChem Research Laboratories, Inc.
P.O. Box 12
Princeton, New Jersey 08540
ATTN: Library

63. Aerojet Liquid Rocket Company
P.O. Box 13222
Sacramento, California 95813
ATTN: Technical Information Center

64. Aeronautical Research Association
of Princeton
50 Washington Road
Princeton, New Jersey 08540
ATTN: Dr. C. Donaldson

65. Aeroprojects, Inc.
West Chester
Pennsylvania 19380

66. The Aerospace Corporation
P.O. Box 92957
Los Angeles, California 90009
ATTN: Mr. Alexander Muraszew

67. Atlantic Research Corporation
5390 Cherokee Avenue
Alexandria, Virginia 22314
ATTN: Dr. Andrej Macek

68. Atlantic Research Corporation
5390 Cherokee Avenue
Alexandria, Virginia 22314
ATTN: Librarian

69. Atlantic Research Corporation
5390 Cherokee Avenue
Alexandria, Virginia 22314
ATTN: Dr. Kermit E. Woodcock
Manager, Propulsion

70. Avco Everett Research Laboratory
Everett, Massachusetts 02149
ATTN: Librarian

71. Avco Lycoming Corporation
550 South Main Street
Stratford, Connecticut 06497
ATTN: Mr. John W. Schrader

72. Ballistics Research Laboratory
Commanding Officer
Aberdeen Proving Ground, Maryland 21005
ATTN: Library

73. Battelle
Columbus Laboratories
505 King Avenue
Colubmus, Ohio 43201
ATTN: Mr. Abbott A. Putnam
Atmospheric Chemistry &
Combustion Systems Division

74. Beech Aircraft Corporation
9709 East Central
Wichita, Kansas 67201
ATTN: William M. Byrne, Jr.

75. Bell Aerospace Company
P.O. Box 1
Buffalo, New York 14240
ATTN: Technical Library

76. Bureau of Mines
Bartlesville Energy Research Center
Box 1398
Bartlesville, Oklahoma 74003

77. Calspan Corporation
4455 Genessee Street
Buffalo, New York 14221
ATTN: Head Librarian

78. Computer Genetics Corporation
Wakefield, Massachusetts 01880
ATTN: Mr. Donald Leonard
Technical Director

79. Convair Aerospace Division
Manager of Propulsion
P.O. Box 748
Fort Worth, Texas 76101
ATTN: L. H. Schreiber

80. Detroit Diesel Allison Division
P.O. Box 894
Indianapolis, Indiana 46206
ATTN: Dr. Sanford Fleeter

81. Dynalysis of Princeton
20 Nassau Street
Princeton, New Jersey 08540
ATTN: Dr. H.J. Herring

82. Fairchild Industries
Fairchild Republic Division
Farmingdale, New York 11735
ATTN: Engineering Library

83. Flame Research, Inc.
P.O. Box 10502
Pittsburgh, Pennsylvania 15235
ATTN: Dr. John Manton

84. Forest Fire and Engineering Research
Pacific Southwest Forest & Range
Experiment Station
P.O. Box 245
Berkeley, California 94701
ATTN: Assistant Director

85. Garrett Corporation
AiResearch Manufacturing Company
Sky Harbor Airport
402 South 36th Street
Phoenix, Arizona 85034
ATTN: Mr. Aldo L. Romanin, Mgr.
Aircraft Propulsion Engine
Product Line

86. General Dynamics
Electro Dynamic Division
P.O. Box 2507
Pomona, California 91766
ATTN: Library MZ 620

87. General Dynamics
P.O. Box 748
Fort Worth, Texas 76101
ATTN: Technical Library MZ 2246

88. General Electric Company
AEG Technical Information Center
Mail Drop N-32, Building 700
Cincinnati, Ohio 45215
ATTN: J.J. Brady

89. General Electric Company
SPO-Bldg, 174AE
1000 Western Avenue
West Lynn, Massachusetts 01910
ATTN: Mr. W. Bruce Gist

90. General Electric Space Sciences Lab
Valley Forge Space Technology Center
Room M-9144
P.O. Box 8555
Philadelphia, Pennsylvania 19101
ATTN: Dr. Theodore Baurer

91. General Motors Corporation
Detroit Diesel Allison Division
P.O. Box 894
Indianapolis, Indiana 46206
ATTN: Mr. P.C. Tram

92. General Motors Technical Center
Passenger Car Turbine Development
General Motors Engineering Staff
Warren, Michigan 48090
ATTN: T.F. Nagey, Director

93. Grumman Aerospace Corporation
Manager Space Vehicle Development
Bethpage, New York 11714
ATTN: Mr. O.S. Williams

94. Mr. Daniel L. Harshman
11131 Embassy Drive
Cincinnati, Ohio 45240

95. Hercules Incorporated
Allegany Ballistics Laboratory
P.O. Box 210
Cumberland, Maryland 21502
ATTN: Mrs. Louise S. Derrick
Librarian

96. Hercules Incorporated
P.O. Box 98
Magna, Utah 84044
ATTN: Library 100-H

97. LTV Vought Aeronautics Company
Flight Technology, Project Engineer
P.O. Box 5907
Dallas, Texas 75222
ATTN: Mr. James C. Utterback

98. Lockheed Aircraft Corporation
Lockheed Missiles and Space Company
Huntsville, Alabama 35804
ATTN: John M. Banefield
Supervisor Propulsion

99. Lockheed-Georgia Company
Dept. 72-47, Zone 259
Marietta, Georgia 30060
ATTN: William A. French

100. Lockheed Missiles and Space Company
3251 Hanover Street
Palo Alto, California 94304
ATTN: Palo Alto Library 52-52

101. Lockheed Propulsion Company
Scientific and Technical Library
P.O. Box 111
Redlands, California 92373
ATTN: Head Librarian

102. Los Alamos Scientific Laboratory
P.O. Box 1663
Los Alamos, New Mexico 97544
ATTN: J. Arthur Freed

103. The Marquardt Company
CCI Aerospace Corporation
16555 Saticoy Street
Van Nuys, California 91409
ATTN: Library

104. Martin-Marietta Corporation
P.O. Box 179
Denver, Colorado 90201
ATTN: Research Library 6617

105. Martin-Marietta Corporation
Orlando Division
P.O. Box 5837
Orlando, Florida 32805
ATTN: Engineering Library, mp-30

106. McDonnell Aircraft Company
P.O. Box 516
St. Louis, Missouri 63166
ATTN: Research & Engineering Library
Dept. 218 - Bldg. 101

107. McDonnell Douglas Corporation
Project Propulsion Engineer
Dept. 243, Bldg. 66, Level 25
P.O. Box 516
St. Louis, Missouri 63166
ATTN: Mr. William C. Paterson

108. McDonnell Douglas Astronautics Company
5301 Bolsa Avenue
Huntington Beach, California 92647
ATTN: A3-328 Technical Library

109. Nielsen Engineering and Research, Inc.
510 Clyde Avenue
Mountain View, California 94040
ATTN: Dr. Jack N. Nielsen

110. Northrop Corporation
Ventura Division
1515 Rancho Conejo Boulevard
Newbury Park, California 91230
ATTN: Technical Information Center

111. Mr. J. Richard Perrin
16261 Darcia Avenue
Encino, California 91316

112. Philco-Ford Corporation
Aeronutronic Division
Ford Road
Newport Beach, California 92663
ATTN: Technical Information Center

113. Pratt and Whitney Aircraft
Project Engineer, Advanced
Military System
Engineering Department - 2B
East Hartford, Connecticut 06108
ATTN: Mr. Donald S. Rudolph

114. Pratt and Whitney Aircraft Division
United Aircraft Company
400 South Main Street
East Hartford, Connecticut 06108
ATTN: Mr. Dana B. Waring
Manager-Product Technology

115. Pratt and Whitney Aircraft
Program Manager, Advanced
Military Engineer
Engineering Department - 2B
East Hartford, Connecticut 06108
ATTN: Dr. Robert I. Strough

116. Pratt and Whitney Aircraft
Florida Research and Development Company
P.O. Box 2691
West Palm Beach, Florida 33402
ATTN: Mr. William R. Alley
Chief of Applied Research

117. Rocket Research Corporation
11441 Willow Road
Redmond, Washington 98052
ATTN: Thomas A. Groudle

118. Rocketdyne Division
North American Rockwell
6633 Canoga Avenue
Canoga Park, California 91304
ATTN: Technical Information Center
D 596-108

119. Sandia Laboratories
P.O. Box 969
Livermore, California 94550
ATTN: Dr. Dan Hartley, Div. 8115

120. Sandia Laboratories
Livermore, California 94550
ATTN: Robert Gallagher

121. Sandia Laboratories
P.O. Box 5800
Albuquerque, New Mexico 87115
ATTN: Technical Library, 3141

122. Solar
2200 Pacific Highway
San Diego, California 92112
ATTN: Librarian

123. Standard Oil Company (Indiana)
P.O. Box 400
Naperville, Illinois 60540
ATTN: R. E. Pritz

124. Stauffer Chemical Company
Richmond, California 94802
ATTN: Dr. J. H. Morgenthaler

125. Teledyne CAE
1330 Laskey Road
Toledo, Ohio 43601
ATTN: Technical Library

126. TRW Systems
One Space Park
Redondo Beach, California 90278
ATTN: Mr. F.E. Fendell (R1/1004)

127. TRW Systems Group
One Space Park
Bldg. 0-1 Room 2080
Redondo Beach, California 90278
ATTN: Mr. Donald H. Lee Manager

128. United Technologies Research Center
East Hartford, Connecticut 06108
ATTN: Librarian

129. Valley Forge Sapce Technology Center
P.O. Box 8555
Philadelphia, Pennsylvania 19101
ATTN: Dr. Bert Zauderer

130. Vought Missiles and Space Company
P.O. Box 6267
Dallas, Texas 75222
ATTN: Library - 3-41000

131. Boston College
Department of Chemistry
Chestnut Hill, Massachusetts 02167
ATTN: Rev. Donald MacLean, S.J.
Associate Professor

132. Brown University
Division of Engineering
Box D
Providence, Rhode Island 02912
ATTN: Dr. R. A. Dobbins

133. California Institute of Technology
Department of Chemical Engineering
Pasadena, California 91109
ATTN: Professor W. H. Corcoran

134. California Institute of Technology
Jet Propulsion Laboratory
4800 Oak Grove Drive
Pasadena, California 91103
ATTN: Library

135. University of California, San Diego
Dept. of Engineering Physics
P.O. Box 109
La Jolla, California 92037
ATTN: Professor S.S. Penner

136. University of California
School of Engineering and
Applied Science
7513 Boelter Hall
Los Angeles, California 90024
ATTN: Engineering Reports Group

137. University of California
Lawrence Radiation Laboratory
P.O. Box 808
Livermore, California 94550
ATTN: Technical Information Dept. L-3

138. University of California
General Library
Berkeley, California 94720
ATTN: Documents Department

139. Case Western Reserve University
10900 Euclid Avenue
Cleveland, Ohio 44106
ATTN: Sears Library - Reports
Department

140. Case Western Reserve University
Division of Fluid Thermal and
Aerospace Sciences
Cleveland, Ohio 44106
ATTN: Professor Eli Reshotko

141. Colorado State University
Engineering Research Center
Fort Collins, Colorado 80521
ATTN: Mr. V. A. Sandborn

142. The University of Connecticut
Department of Mechanical Engineering
U-139
Storrs, Connecticut 06268
ATTN: Professor E. K. Dabora

143. Cooper Union
School of Engineering and Science
Cooper Square
New York, New York 10003
ATTN: Dr. Wallace Chintz
Associate Professor of ME

144. Cornell University
Department of Chemistry
Ithaca, New York 14850
ATTN: Professor Simon H. Bauer

145. Franklin Institute Research Laboratories
Philadelphia, Pennsylvania 19103
ATTN: Dr. G.P. Wachtell

146. George Washington University
Washington, D.C. 20052
ATTN: Dr. Robert Goulard
Dept. of Civil, Mechanical and
Environmental Engineering

147. George Washington University Library
Washington, D.C. 20006
ATTN: Reports Section

148. Georgia Institute of Technology
Atlanta, Georgia 30332
ATTN: Price Gilbert Memorial Library

149. Georgia Institute of Technology
School of Aerospace Engineering
Atlanta, Georgia 30332
ATTN: Dr. Ben T. Zinn

150. University of Illinois
Department of Energy Engineering
Box 4348
Chicago, Illinois 60680
ATTN: Professor Paul H. Chung

151. University of Illinois
College of Engineering
Department of Energy Engineering
Chicago, Illinois 60680
ATTN: Dr. D. S. Hacker

152. The Johns Hopkins University
Applied Physics Laboratory
Johns Hopkins Road
Laurel, Maryland 20810
ATTN: Chemical Propulsion
Information Agency

153. The Johns Hopkins University
Applied Physics Laboratory
Johns Hopkins Road
Laurel, Maryland 20810
ATTN: Document Librarian

154. The Johns Hopkins University
Applied Physics Laboratory
Johns Hopkins Road
Laurel, Maryland 20810
ATTN: Dr. A. A. Westenberg

155: University of Kentucky
Department of Mechanical Engineering
Lexington, Kentucky 40506
ATTN: Dr. Robert E. Peck

156. Massachusetts Institute of Technology
Department of Chemical Engineering
Cambridge, Massachusetts 02139
ATTN: Dr. Jack B. Howard

157. Massachusetts Institute of Technology
Libraries, Room 14 E-210
Cambridge, Massachusetts 02139
ATTN: Technical Reports

158. Massachusetts Institute of Technology
Room 10-408
Cambridge, Massachusetts 02139
ATTN: Engineering Technical Reports

159. Massachusetts Institute of Technology
Dept. of Mechanical Engineering
Room 3-350
Cambridge, Massachusetts 02139
ATTN: Dr. M. Cardillo

160. Massachusetts Institute of Technology
Dept. of Mechanical Engineering
Room 3-246
Cambridge, Massachusetts 02139
ATTN: Professor James Fay

161. Midwest Research Institute
425 Volker Boulevard
Kansas City, Missouri 64100
ATTN: Dr. T. A. Milne

162. New Mexico State University
Dept. of Mechanical Engineering
Box 3450
Las Cruces, New Mexico 88003
ATTN: Dr. Dennis M. Zallen

163. New York Institute of Technology
Wheatley Road
Old Westbury, New York 11568
ATTN: Dr. Fox

164. University of North Carolina
Periodicals and Serials Division
Drawer 870 Library
Chapel Hill, North Carolina 27514
ATTN: Mr. Stephen Berk

165. University of Notre Dame
Serials Record
Memorial Library
Notre Dame, Indiana 46556
ATTN: B. McIntosh

166. University of Notre Dame
College of Engineering
Notre Dame, Indiana 46556
ATTN: Dr. Stuart T. McComas
Assistant Dean for Research
and Special Projects

167. Ohio State University
Dept. of Chemical Engineering
140 West 19th Avenue
Columbus, Ohio 43210
ATTN: Dr. Robert S. Brodkey

168. The Pennsylvania State University
Room 207, Old Main Building
University Park, Pennsylvania 16802
ATTN: Office of Vice President
for Research

169. Princeton University
Dept. of Acrospace and Mechanical
Sciences
James Forrestal Campus
Princeton, New Jersey 08540
ATTN: Dr. Martin Summerfield

170. Princeton University
James Forrestal Campus Library
P.O. Box 710
Princeton, New Jersey 08540
ATTN: V. N. Simosko, Librarian

171. Rice University
Welch Professor of Chemistry
Houston, Texas 77001
ATTN: Dr. Joseph L. Franklin

172. University of Rochester
Dept. of Chemical Engineering
Rochester, New York 14627
ATTN: Dr. John R. Ferron

173. Stanford University
Dept. of Aeronautics and Astronautics
Stanford, California 94305
ATTN: Dr. Walter G. Vincenti

174. State University of New York - Buffalo
Dept. of Mechanical Engineering
228 Parker Engineering Building
Buffalo, New York 14214
ATTN: Dr. George Rudinger

175. Stevens Institute of Technology
Department of Mechanical Engineering
Castle Point Station
Hoboken, New Jersey 07030
ATTN: Professor Fred Sisto

176. University of Virginia
Department of Aerospace Engineering
School of Engineering and Applied Science
Charlottesville, Virginia 22901
ATTN: Dr. John E. Scott

177. University of Virginia
Science/Technology Information Center
Charlottesville, Virginia 22901
ATTN: Dr. Richard H. Austin

178. Yale University
Mason Laboratory
9 Hillhouse Avenue
New Haven, Connecticut 06520
ATTN: Professor Peter P. Wegener

FOREIGN INSTITUTIONS

179. A/S Kongsberg Vaapenfabrikk
Gas Turbine Division
3601 Konsber, NORWAY
ATTN: R.E. Stanley
Senior Aerodynamicist

180. Conservatoire National des Arts
et Metiers
292, Rue Saint'Martin
75141 Paris Cedex 03, FRANCE
ATTN: Professor J. Gossee
Chaire de Thermique

181. DFVLR-Forschungszentrum Gottingen
Institut Fur Stromungsmechanik
Abteilung Theoretische Gashynamik
D-3400 Gottingen
Bunsenstrabe 10, GERMANY
ATTN: Professor Klaus Oswatitsch

182. Ecole Royale Militaire
30 Avenue de la Resaissance
Bruxelles B-1040, BELGIUM
ATTN: Professor Emile Tits

183. Fysisch Laboratorium
Fijksuniversiteit Utrecht
Sorbonnelaan, Utrecht,
THE NETHERLANDS
ATTN: Dr. F. Van der Valk

184. Imperial College
Department of Chemical Engineering
London SW7, ENGLAND
ATTN: Professor F. J. Weinberg

185. Imperial College of Science
and Technology
Department of Mechanical Engineering
Exhibition Road
London, SW7, ENGLAND
ATTN: Professor Gaydon

186. Imperial College of Science
and Technology
Department of Mechanical Engineering
Exhibition Road
London SW7, ENGLAND
ATTN: D. B. Spalding

187/1 Laboratoire de Mecanique des Fluides
36, Route de Dardilly, 36
B.P. No. 17
69130 Ecully, FRANCE
ATTN: G. Assassa

187/2 Laboratoire de Mecanique des Fluides
Ecole Centrale Lyonnaise
36, Route de Dardilly
69130 Ecully, FRANCE
ATTN: Dr. K. Papiliou

188. Ministry of Defense
Main Building, Room 2165
Whitehall Gardens
London SW1, ENGLAND
ATTN: Mr. L.D. Nicholson ED, idc
Vice Controller of Aircraft
Procurement Executive

189. Mitglied des Vorstands der Fried
Krumpp CmbH
43 Essen, Altendorferstrabe 103
GERMANY
ATTN: Professor Dr.-Ing.
Wilhelm Dettmering

190. National Aerospace (NLR)
Voorsterweg 31
Noord-Oost-Polder-Emmelord
THE NETHERLANDS
ATTN: Mr. F. Jaarsma

191. National Research Council
Division of Mechanical Engineering
Montreal Road, Ottawa
Ontario, CANADA KIA OR6
ATTN: Dr. R.B. Whyte

192. Nissan Motor Co., LTD.
3-5-1, Momoi, Suginami-Ku
Tokyo, JAPAN 167
ATTN: Dr. Y. Toda

193. Norweigian Defense Research Establishment
Superintendent NDRE
P.O. Box 25
2007 Kjeller, NORWAY
ATTN: Mr. T. Krog

194. ONERA
Energie and Propulsion
29 Avenue de la Division Leclure
92 Chatillon sous Bagneux, FRANCE
ATTN: Mr. M. Barrere

195. ONERA
Energie and Propulsion
29 Avenue de la Division Leclure
92 Chatillon sous Bagneux, FRANCE
ATTN: Mr. J. Fabri

196. ONERA
Energie and Propulsion
29 Avenue de la Division Leclure
92 Chatillon sous Bagneux, FRANCE
ATTN: Mr. Viaud

197. ONERA-DED
External Relations and Documentation
Department
29, Avenue de la Division Leclure
92320 Chatillon, sous Bagneux, FRANCE
ATTN: Mr. M. Salmon

198. Orta Dogu Teknik Universities
Mechanical Engineering Department
Ankara, TURKEY
ATTN: Professor H. Sezgen

199. Queen Mary College
Department of Mechanical Engineering
Thile Eld Road
London E1, ENGLAND
ATTN: Professor M. W. Thring

200. Rolls-Royce (1971) Limited
Derby Engine Division
P.O. Box 31
Derby DE2 8BJ
London, ENGLAND
ATTN: C. Freeman, Installation
Research Department

201. Rome University
Via Bradano 28
00199 Rome, ITALY
ATTN: Professor Gaetano Salvatore

202. Sener
Departamentao de Investigation
Km. 22.500 de la antigua carretera
Madrid - Barcelona, SPAIN
ATTN: Mr. J. T. Diez Roche

203. Service Technique Aeronautique Moteurs
4 Avenue de la Parte d'Issy
75753 Paris Cedex 15, FRANCE
ATTN: Mr. M. Pianko, Ing. en chef

204. The University of Sheffield
Dept. of Chemical Engineering
and Fuel Technology
Mappin Street, Sheffield S1 3JD
ENGLAND
ATTN: Dr. Norman Chigier

205. Sophia University
Science and Engineering Faculty
Kioi 7 Tokyo-Chiyoda JAPAN 102
ATTN: Professor M. Susuki

206. The University of Sydney
Dept. of Mechanical Engineering
N.S.W. 2006
Sydney, AUSTRALIA
ATTN: Professor R. W. Bilger

207. Technical University of Denmark
Fluid Mechanics Department
Building 404 2800 Lyngby
DK-DENMARK
ATTN: Professor K. Refslund

208. University of Leeds
Leeds, ENGLAND
ATTN: Professor Dixon-Lewis

209. Universite de Poitiers Laboratoire
D'energetique et de Detonique
(L.A. au C.N.R.S. No. 193)
ENSMA - 86034 Poitiers, FRANCE
ATTN: Professor N. Manson

210. University of Tokyo
Department of Reaction Chemistry
Faculty of Engineering
Bunkyo-ku
Tokyo, JAPAN 113
ATTN: Professor T. Hikita

211. Vrije Universiteit Brussel
Fac. Toeg. Wetenshch.
A. Buyllaan 105
1050 Brussels, BELGIUM
ATTN: Ch. Hirsch

PROJECT SQUID CONTRACTORS
1975-76 and 1976-77 (New)

212. AeroChem Research Laboratory, Inc.
Reaction Kinetics Group
P.O. Box 12
Princeton, New Jersey 08540
ATTN: Dr. Arthur Fontijn

213. Aeronautical Research Associates of
Princeton, Inc.
P.O. Box 2229
50 Washington Road
Princeton, New Jersey 08540
ATTN: Dr. Ashok K. Varma

214. California Institute of Technology
Div. of Engineering and
Applied Science
Mail Stop 205-50
Pasadena, California 91109
ATTN: Dr. Anatol Roshko

215. Case Western Reserve University
Div. of Fluid, Thermal and Aerospace
Sciences
Cleveland, Ohio 44106
ATTN: Dr. J.S. T'ien

216. Colorado State University
Engineering Research Center
Foothills Campus
Fort Collins, Colorado 80521
ATTN: Dr. Willy Z. Sadeh

217. General Electric Company
Corporate Research and Development
P.O. Box 8
Schenectady, New York 12301
ATTN: Dr. Marshall Lapp

218. Massachusetts Institute of Technology
Chemistry Department, Room 6-123
77 Massachusetts Avenue
Cambridge, Massachusetts 02139
ATTN: Dr. John Ross

219. Michigan State University
Department of Mechanical Engineering
East Lansing, Michigan 48824
ATTN: Dr. John Foss

220. Pennsylvania State University
Applied Research Laboratory
University Park, Pennsylvania 16802
ATTN: Dr. Edgar P. Bruce

221. Polytechnic Institute of New York
Department of Aerospace Engineering and Applied Mechanics
Farmingdale, New York 11735
ATTN: Dr. Samuel Lederman

222. Southern Methodist University
Thermal and Fluid Sciences Center
Institute of Technology
Dallas, Texas 75275
ATTN: Dr. Roger L. Simpson

223. Stanford University
Mechanical Engineering Department
Stanford, California 94305
ATTN: Dr. James P. Johnston

224. Stanford University
Mechanical Engineering Department
Stanford, California 94305
ATTN: Dr. S. J. Kline

225. Stanford University
Mechanical Engineering Department
Stanford, California 94305
ATTN: Dr. Sidney Self

226. TRW Systems
Engineering Sciences Laboratory
One Space Park
Redondo Beach, California 90278
ATTN: Dr. J. E. Broadwell

227. United Technologies Research Center
400 Main Street
East Hartford, Connecticut 06108
ATTN: Mr. Franklin O. Carta

228. United Technologies REsearch Center
400 Main Street
East Hartford, Connecticut 06108
ATTN: Dr. Alan C. Eckbreth

229. University of California - San Diego
Department of Aerospace and Mechanical Engineering
La Jolla, California 92037
ATTN: Dr. Paul Libby

230. University of Colorado
Department of Aerospace Engineering Sciences
Boulder, Colorado 80304
ATTN: Dr. Mahinder S. Uberoi

231. University of Michigan
Department of Aerospace Engineering
Ann Arbor, Michigan 48105
ATTN: Dr. T. C. Adamson, Jr.

232. University of Michigan
Department of Aerospace Engineering
Ann Arbor, Michigan 48105
ATTN: Dr. Martin Sichel

233. University of Missouri - Columbia
Department of Chemistry
Columbia, Missouri 65201
ATTN: Dr. Anthony Dean

234. University of Southern California
Department of Aerospace Engineering
University Park
Los Angeles, California 90007
ATTN: Dr. F. K. Browand

235. University of Washington
Department of Mechanical Engineering
Seattle, Washington 98195
ATTN: Dr. F.B. Gessner

236. Virginia Polytechnic Institute and State University
Mechanical Engineering Department
Blacksburg, Virginia 24601
ATTN: Dr. Walter F. O'Brien, Jr.

237. Virginia Polytechnic Institute and State University
Mechanical Engineering Department
Blacksburg, Virginia 24061
ATTN: Dr. Hal L. Moses

238. Yale University
Engineering and Applied Science
Mason Laboratory
New Haven, Connecticut 06520
ATTN: Dr. John B. Fenn

PURDUE UNIVERSITY

239. School of Aeronautics and Astronautics
Grissom Hall
West Lafayette, Indiana 47907
ATTN: Library

240. School of Mechanical Engineering
Mechanical Engineering Building
West Lafayette, Indiana 47907
ATTN: Library

241-250. Purdue University Advisors

Unclassified

SECURITY CLASSIFICATION OF THIS PAGE (*When Data Entered*)

REPORT DOCUMENTATION PAGE		READ INSTRUCTIONS BEFORE COMPLETING FORM
1. REPORT NUMBER POLY M/AE Report No. 76-10	2. GOVT ACCESSION NO.	3. RECIPIENT'S CATALOG NUMBER 9 Interim Rept.
4. TITLE (*and Subtitle*) 6 TEMPERATURE, CONCENTRATION VELOCITY AND TURBULANCE MEASUREMENTS IN JETS AND FLAMES,		5. TYPE OF REPORT & PERIOD COVERED Scientific - Interim
		6. PERFORMING ORG. REPORT NUMBER 15
7. AUTHOR(s) 10 S. Lederman, A. Celentano ~~and~~ J. Glaser		8. CONTRACT OR GRANT NUMBER(s) N00014-75-C-1143 Subcontract 8960-5
9. PERFORMING ORGANIZATION NAME AND ADDRESS Polytechnic Institute of New York Aerodynamics Laboratories Route 110, Farmingdale, N.Y. 11735		10. PROGRAM ELEMENT, PROJECT, TASK AREA & WORK UNIT NUMBERS
11. CONTROLLING OFFICE NAME AND ADDRESS Project SQUID Thermal Science & Propulsion Center Purdue University West Lafayette, Indiana 47907	11	12. REPORT DATE December 1976
		13. NUMBER OF PAGES 60
14. MONITORING AGENCY NAME & ADDRESS (*if different from Controlling Office*) Office of Naval Research Power Program, Code 473 Dept. of the Navy Arlington, Virginia 22217	12 60p.	15. SECURITY CLASS. (*of this report*) Unclassified
		15a. DECLASSIFICATION/DOWNGRADING SCHEDULE

16. DISTRIBUTION STATEMENT (*of this Report*)

Approved for public release; distribution unlimited.

14 SQUID-PIB-34-PU

17. DISTRIBUTION STATEMENT (*of the abstract entered in Block 20, if different from Report*)

18. SUPPLEMENTARY NOTES

19. KEY WORDS (*Continue on reverse side if necessary and identify by block number*)

Raman	Turbulence
Doppler	Flame
Concentration	Jet
Temperature	
Velocity	

20. ABSTRACT (*Continue on reverse side if necessary and identify by block number*)

The recently developed Laser Raman, Laser Doppler Velocimetry and Coherent Antistokes Raman Scattering are applied to the diagnostics of flow fields and flames. The concentration of species in a cold jet, and the velocities are measured and compared to measurements using standard techniques. The Raman and LDV techniques are then applied to diffusion flames. Experimental results concerning concentration of species, temperature, velocities and

next page

DD FORM 1 JAN 73 1473 EDITION OF 1 NOV 65 IS OBSOLETE

Unclassified

SECURITY CLASSIFICATION OF THIS PAGE (*When Data Entered*)

403617

Unclassified
SECURITY CLASSIFICATION OF THIS PAGE(When Data Entered)

20. Abstract (Continued)

turbulent intensities are obtained simultaneously. The latter are obtained from the LDV data as well as the concentration data. It is seen that by proper processing of the concentration data an indication and a measure of the turbulent intensity may be obtained. It is further shown that from the simultaneously acquired concentration data a parameter of major importance in turbulence modeling, the "mixedness" parameter or the cross correlation function may be directly measured.

Unclassified
SECURITY CLASSIFICATION OF THIS PAGE(When Data Entered)